Bioactive Materials 28 (2023) 511–536

Contents lists available at ScienceDirect

Bioactive Materials

journal homepage: www.keaipublishing.com/en/journals/bioactive-materials

Review article

Biomaterials / bioinks and extrusion bioprinting

X.B. Chen [a,b,*], A. Fazel Anvari-Yazdi [b], X. Duan [b], A. Zimmerling [b], R. Gharraei [b], N.K. Sharma [a], S. Sweilem [c], L. Ning [c]

[a] Department of Mechanical Engineering, University of Saskatchewan, 57 Campus Dr, S7K 5A9, Saskatoon, Canada
[b] Division of Biomedical Engineering, University of Saskatchewan, 57 Campus Dr, Saskatoon, S7K 5A9, Canada
[c] Department of Mechanical Engineering, Cleveland State University, Cleveland, OH, 44115, USA

ARTICLE INFO

Keywords:
3D bioprinting
Extrusion
Bioinks
Biomaterials
Tissue engineering

ABSTRACT

Bioinks are formulations of biomaterials and living cells, sometimes with growth factors or other biomolecules, while extrusion bioprinting is an emerging technique to apply or deposit these bioinks or biomaterial solutions to create three-dimensional (3D) constructs with architectures and mechanical/biological properties that mimic those of native human tissue or organs. Printed constructs have found wide applications in tissue engineering for repairing or treating tissue/organ injuries, as well as in vitro tissue modelling for testing or validating newly developed therapeutics and vaccines prior to their use in humans. Successful printing of constructs and their subsequent applications rely on the properties of the formulated bioinks, including the rheological, mechanical, and biological properties, as well as the printing process. This article critically reviews the latest developments in bioinks and biomaterial solutions for extrusion bioprinting, focusing on bioink synthesis and characterization, as well as the influence of bioink properties on the printing process. Key issues and challenges are also discussed along with recommendations for future research.

1. Introduction

Biomaterial solutions can be synthesized with living cells and/or biomolecules (such as growth factors) to form bioinks for the printing of functional scaffolds or constructs for tissue engineering and regenerative medicine. The printing process deposits the bioinks or biomaterial solutions in a predesigned manner to build up three-dimensional (3D) structures in a layer-by-layer fashion (Fig. 1) [1–3]. If the printing process involves living cells, it is commonly referred to as bioprinting and the printed structures are referred to as constructs, while if no living cells are involved the process is simply termed printing and the printed structures as scaffolds. In this paper, we refer to bioprinting and its subsequent constructs unless otherwise specified. Among the bioprinting techniques developed to date, extrusion bioprinting, which employs mechanical forces to extrude the bioink or biomaterial solution, has been widely used in the fabrication of constructs [1,4]. The mechanical forces employed in extrusion bioprinting can be classified into three categories: pneumatic, piston, and screw-driven (Fig. 2). The pneumatic-driven printing process utilizes pressurized air to drive the bioink or biomaterial solution out of the needle and, as such, deposition of the bioink or biomaterial solution is controlled by regulating the pressure of compressed air. Due to the advantages of its simple operation and ease of maintenance, pneumatic-driven printing has been widely used. In the piston or screw-driven printing process, the bioink or biomaterial solution inside the syringe is mechanically extruded by a piston or a screw [5]. Both piston- and screw-driven printing can provide larger mechanical forces and allow for more direct control over the flow of bioink compared to pneumatic-driven printing [5–9].

Bioprinted constructs have found wide applications related to biomedical engineering, including tissue engineering (TE) and combating infectious diseases (CID). In TE, bioprinted constructs are cultured in bioreactors and grown into functional 'artificial' tissue/organ substitutes, which are then implanted into patients to help repair or treat tissue/organ injuries [1,2]. In CID, bioprinted constructs are created to mimic human tissue/organs (e.g., human lung), serving as in vitro (out of body) tissue or virus-disease models to test/validate newly developed therapeutics and vaccines prior to their use in humans [9–12]. For these applications, several functional requirements including architectural, mechanical, and biological properties have been identified as crucial. The architectural properties of a construct refer to

Peer review under responsibility of KeAi Communications Co., Ltd.
* Corresponding author
E-mail address: xbc719@mail.usask.ca (X.B. Chen).

https://doi.org/10.1016/j.bioactmat.2023.06.006
Received 24 February 2023; Received in revised form 19 May 2023; Accepted 8 June 2023

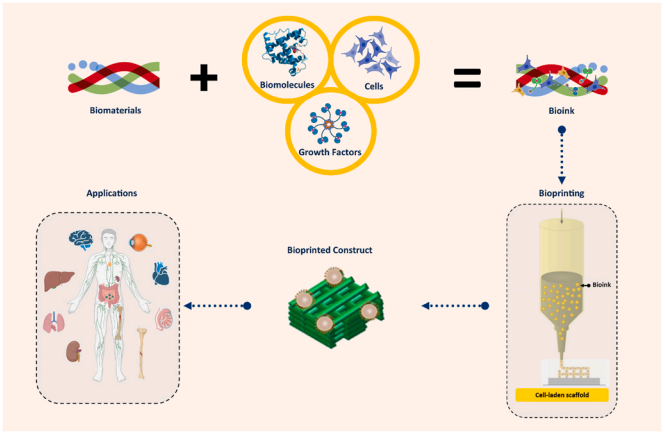

Fig. 1. Constructs printed from bioinks and applications.

its external geometry and internal structure, with the external geometry aiming to mimic that of the tissue/organ to be repaired and its internal structure requiring a high degree of porosity for cell growth/movement, transport of nutrients into the construct, and removal of metabolic wastes out of the construct during the healing process. The mechanical properties of a construct refer to its mechanical strength and degradation. Notably, the materials of a construct, once implanted, degrade as the tissue regenerates within it. As a result, the mechanical properties of constructs are dynamic, with the decrease in biomaterial strength caused by degradation being combatted by an increase in mechanical strength due to tissue regeneration. Eventually, the mechanical properties of the construct should be similar to those of the tissue/organ being repaired throughout regeneration. The biological properties of a construct refer to its ability to support cell growth/functions (such as cell attachment, proliferation, and differentiation) and tissue regeneration, with limited or no negative effects (such as inflammation) on the host system (i.e., animal or human) in which the tissues/organs are being repaired.

Successful bioprinting of constructs and their subsequent success in applications relies on the properties of the formulated bioinks or biomaterial solutions, including the rheological, mechanical, and biological properties, as well as the selected bioprinting process. Over the last two decades, advances in biomaterials/bioinks and extrusion printing techniques has allowed for creation of diverse and complicated constructs for a wide range of tissue engineering applications, including repair of damaged skin [13,14], cartilage [15–17], bones [18], nerves [19,20], teeth [21,22], and spinal cords [23,24], as well as the treatment of corneal blindness [25], heart attacks and strokes [26–28]. In this paper, we review the recent development of bioinks and biomaterial solutions in reference to important properties for extrusion printing, with a focus on biomaterial and bioink synthesis, characterization, extrusion bioprinting of constructs, and advances in extrusion bioprinting. Key issues and challenges are also discussed along with recommendations for future research.

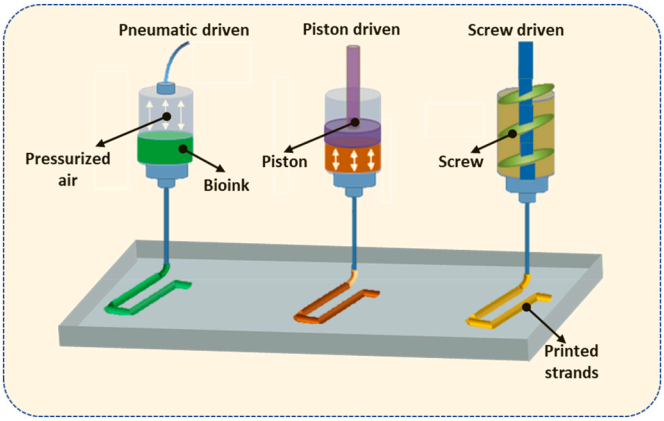

Fig. 2. Schematic of pneumatic-, piston-, and screw-driven printing.

2. Biomaterials and bioinks

2.1. Biomaterials

Biomaterial solutions and/or bioinks used for bioprinting have been synthesized widely from polymers. Polymers are organic biomaterials possessing long chains with high water contents, thus being able to provide a hydrated tissue-like environment that supports cell functions (including cell attachment, proliferation, and differentiation) and tissue regeneration [29]. Polymers are either natural or synthetic; natural polymers have the intrinsic capability to support cell functions, while synthetic polymers are usually biologically inert, but exhibit strong and robust mechanical properties.

2.1.1. Natural polymers

Alginate, also known as alginic acid, is a water-soluble polysaccharide primarily derived from brown seaweed. This family of natural polymers is comprised of β-D-mannuronic acid (M) and α-L-guluronic acid (G). The monomers can appear in homopolymeric blocks of consecutive G-residues (G-blocks), consecutive M-residues (M-blocks), or alternating M − and G-residues (MG-blocks). Varying amounts of G and M blocks in alginate result in molecular weights that can range from 50 to 100,000 kDa. Alginate has been extensively used in extrusion bioprinting due to its ease of printing to form 3D structures, compatibility with ionic cross-linking, along with its water absorbency and low cost [30–32]. Alginate solutions used in bioprinting have demonstrated compatibility with many cell types from different tissues, such as bone, muscle, cartilage, skin, nerve, and blood vessels, as well as functional organs including the heart, liver, kidney, and bladder [33–37]. However, alginate possesses the critical disadvantage of poor cell adhesion. Lack of adhesion molecules in alginate, or transmembrane glycoproteins, significantly reduces the interaction between cells and alginate, thus limiting cell functions. The adhesion properties of alginate can be improved by adding other biomaterials that have inherent capacities for cell attachment [17,33–43] or modifying with special adhesion molecule sequences, such as RGD peptides, that can covalently bond to alginate chains [44].

Chitosan is a common natural polymer found in crustacean shells and fungi cell walls which is derived by alkali deacetylation of chitin It is a linear polysaccharide composed of randomly distributed N-acetyl-D-glucosamine (acetylated unit) and β-(1–4)-linked D-glucosamine (deacetylated unit). Chitosan is readily soluble in dilute acidic medium below its pKa (pH = 6.5) while chitin is insoluble in organic and regular solvents [45]. Chitosan is well known for being relatively cheap with favorable non-toxic, biodegradable, antibacterial, and antifungal properties; as such, it has been used in many medical applications ranging from pharmaceuticals to wound dressings [46–48], as well as in bioprinting [17,49]. As an acid environment is not suitable for cell survival, bioprinting cell-incorporated scaffolds using typical chitosan solutions and living cells is challenging. One way to solve the problem is chemically modifying the properties of chitosan to make it soluble in water, with neutral pH after dissolution [50,51]. The utilization of chitosan is also often limited by its slow gelation rate and poor mechanical properties for bio-printing [50]. These limitations can be alleviated by adding other hydrogels such as gelatin, starch, collagen, pectin and alginate to chitosan solutions to enhance the polymerization rate and structural strength [52–56]. Chitosan has the ability to form crosslinks with a wide range of compounds, including citrates and phosphates like tripolyphosphate (TPP), through an ionotropic process. With other

polyelectrolytes, particularly polyanions such as alginate or hyaluronic acid, chitosan can be effectively crosslinked, thus being suitable for 3D-bioprinting [57].

Agarose is a natural water-soluble polysaccharide that is purified from seaweed (red algae) and can be self-crosslinked and de-crosslinked using temperature control. Typically, agarose solution can be rapidly gelled when the temperature drops to between 26 and 30 °C, which makes it printable, but some challenges remain. Agarose provides limited support of cell growth due to its non-adhesive nature and degrades over time [58]. Because of its inert nature, agarose is often used to form cell aggregates and/or support the differentiation of encapsulated cells [58]. Collagen can be mixed into agarose solutions to increase support of cellular functions such as biosynthesis of proteins and proteoglycans allowing for the incorporation of living cells [59]. Also, agarose has been used as a 'sacrifice biomaterial' in scaffold vascularization due to its thermosensitivity [60]. In this strategy, agarose fibers are printed with a pre-defined pattern, with the functional biomaterials and cells then cast over the fibers and crosslinked. Using temperature control, the agarose fibers can be easily melted and removed, with the patterned channels left behind [60].

Hyaluronic acid (HA) is the most prevalent glycosaminoglycan that exists in the extracellular matrix (ECM) [61]. It is distributed throughout the human body and is predominantly involved in connective, epithelial, and neural tissues. HA stimulates limited inflammatory response and has antigenic potential allowing for its extensive use in clinics as a dermal filler for wound healing while its lubricating properties have allowed for its use as synovial fluid in articular joints [2]. HA is water soluble, with the resulting solution having a high viscosity and as such, it is often used as an assistant material to adjust the viscosity of other biomaterial solutions in bioprinting [39,62,63]. Tunable physical and biological properties make HA a suitable material for incorporating cells [64,65]. HA can gel by covalent crosslinking with hydrazide derivatives, by esterification, or by annealing, but all of these processes take a long time and can be toxic to encapsulated cells [66]. Additionally, gelled HA has poor mechanical properties and is characterized by a rapid degradation rate [66]. To address these shortcomings, HA is normally modified with UV-curable methacrylate (MA) to become photopolymerizable. The HA-MA maintains the crucial biological properties of HA while gaining controllable crosslinking properties, which greatly improves crosslinking efficacy and mechanical stability for scaffold bioprinting applications [66].

Collagen is an abundant, naturally occurring protein in the body that consists of self-aggregating polypeptide chains held together by both hydrogen and covalent bonds. It is the most widely used natural material for tissue scaffolds due to its natural receptors for cell attachment, creating the possibility to directly affect cell adhesion and other functions [67,68]. There are a number of different types of collagens that have been identified; some collagens are more compatible with bioprinting applications than others [69]. The most widely used collagen formations in tissue engineering include collagen type I, II, IV, and V [70]. Among these, collagen type I has been extensively applied in scaffold bioprinting [71,72]. It is dissolvable in faintly acidic aqueous solutions and can be polymerized within 60 min at 37 °C and neutral pH. As such, collagen scaffolds can be printed by controlling the pH and temperature. Collagen scaffolds have been used with diverse cell types, including adipose, bladder, blood vessel, bone, cartilage, heart, liver, nerve, and skin tissues, among many others; however, they face the limitation of inherently poor mechanical properties. To make collagen more suitable for scaffold bioprinting and tissue engineering applications, covalent bonding and irradiation crosslinking methods have been applied along with the thermal polymerization of collagen solutions [71]. Additionally, mixing collagen solution with other materials such as alginate, gelatin, and HA has also been adopted in scaffold bioprinting to improve mechanical properties [71]. For the repair of many hard tissues, such as bone and cartilage, scaffolds made from collagen and synthetic polymers such as polycaprolactone (PCL) and poly(lactic-co-glycolic acid) (PLGA) have often been used, where the synthetic polymers are printed first in a designated pattern as a scaffold frame to provide the mechanical support for the structures and cells and then collagen and cells are subsequently deposited inside the spaces created by the frame to realize the biological functions of the scaffold [70].

Gelatin derived through partial hydrolysis of collagen has advantages such as good biocompatibility, non-immunogenicity, cell-affinity, and complete biodegradability in vivo [73]. Gelatin is widely used for tissue engineering applications as it possesses a similar composition to collagen. Analogous to collagen, gelatin is sensitive to temperature and crosslinked at low temperatures [73]. When the temperature increases to the physiological range or higher, gelation de-crosslinks and shows instability. Therefore, for extrusion-based bioprinting applications, chemicals including metal ions, glutaraldehyde, and other printable materials have been used to improve the printability and stability of gelatin [41–43]. Photo-crosslinkable gelatin hydrogels have been synthesized by chemically modifying gelatin with methacrylamide side groups. Synthesized gelatin methacrylate composite (GelMA) hydrogels have been successfully printed with the help of UV-light and further employed to encapsulate various cell types for the fabrication of tissue-engineered cardiac valves, cartilage, and vessel-like structures [74,75]. The mechanical properties of modified gelatin can be regulated by controlling the gelatin concentration, UV light intensity, or exposure time [74,75].

Fibrin is a fibrous protein that naturally forms in the body during blood coagulation and is also a component of natural ECM [76]. It contains fibrinogen, which is a protein comprised of two sets of three polypeptide chains: Aα, Bβ, and γ chains [77]. Fibrinogen can be gelled to form fibrin hydrogels by adding thrombin, a serine protease that converts fibrinogen into fibrin. Coagulation factor XIII can covalently crosslink with the γ chains in the fibrin polymer to produce a fibrin network that is stable and resists protease degradation. During bioprinting, fibrin can be simply achieved via direct deposition of fibrinogen solution into a mixture containing thrombin and factor XIII [78,79]. Fibrin is a versatile biopolymer with excellent potential in 3D-biofabrication [80]. Fibrin-based scaffolds have an inherent cell adhesion capacity, which encourages many applications based on mixing cells into fibrinogen solutions to build cell-incorporated fibrin constructs that enhance the proliferation [76]. However, the utilization of fibrin scaffolds is limited by their low mechanical stability and rapid degradation [81]. Methods to improve their mechanical properties include using high concentrations of fibrinogen or thrombin during fibrin formation or mixing fibrinogen with other biomaterials that provide better mechanical stability [82]. The rapid degradation rate can be moderated by adding protease inhibitors such as aprotinin into the fibrinogen solutions or culture medium, or by optimizing the printing temperature, calcium ion concentration, and cell density. Building fibrin-based scaffolds by extrusion bioprinting is challenging due to the limited viscosity of fibrinogen solution. Pre-mixed fibrinogen and thrombin solutions have been applied in fibrin-based scaffold fabrication to improve the viscosity of printed solutions [77]. Fibrinogen solutions with a pre-determined ratio of fibrinogen and thrombin are normally prepared at a low temperature (around 0 °C) to moderate the gelation. Other methods to improve the printability of fibrin include mixing fibrinogen with other biomaterials during solution preparation and crosslinking them after with associated crosslinkers for scaffold bioprinting [81,82].

Decellularized extracellular matrix (dECM) is a natural biomaterial obtained through the decellularization of native tissues. Decellularization is a process involving the lysis and removal of cellular components by the perfusion of anionic (e.g., sodium dodecyl sulfate-SDS), nonionic (e.g., Triton-X100) or other mild detergents while preserving the ECM of the tissue [83]. By this process, dECM contains various, yet bioactive, molecules and proteins such as collagen, glycosaminoglycans (GAGs), laminins, elastin, and fibronectin as well as growth factors, which facilitate cell growth and functions [84] and as such, it is promising for use in developing biomimetic tissues and organs

by bioprinting. Recent advances in dECM have allowed for the synthesis of new dECM-based biomaterials compatible with various techniques (including printing) for tissue engineering and medical regeneration of various organs including the heart, kidney, and liver [5]. dECM can be digested into an acidic solution (e.g., HCl and acetic acid) and then neutralized by NaOH. dECM is crosslinkable after incubation at 37 °C due to the presence of collagens. Notably, dECM has weak mechanical properties, which limits its application in hard tissue (such as bone) engineering [85,86]. To address this, other polymers such as PCL are normally used as frameworks to enhance the structural stability [87]. There are still unknowns about the biochemical and structural nature of ECM as well as issues left to be addressed for its processing and applications in bioprinting [84]. Future research studies are urged to develop novel methods/techniques/strategies for minimizing damage to dECM, stabilizing dECM with improved durability, printing dECM to form scaffolds with appropriate architecture and mechanical/biological properties, and re-cellularizing dECM or scaffolds with appropriate cell types including their subsequent cell culture for the formation of functional scaffolds or constructs.

Peptide-based hydrogels are developed through the synthesis and self-assembly of peptides into hydrogels or their structures. To date, a variety of hydrogel structures have been formed through noncovalent forces including hydrogen bonding, electrostatic, and hydrophobic interactions between peptides, or through chemical or enzymatic cross-linking [88,89]. Peptides, formed from amino acids, can be differentiated into short or long chain peptide hydrogels based on the number of –CONH- amide linkages present [88]. These synthesized natural materials are highly bioactive, enabling cell adhesion, proliferation, migration and differentiation, as they are derived from ECM components and can be used to direct further cellular activities [89]. The physiochemical properties of a peptide bioink, including hydrophilicity/hydrophobicity, gelation, release kinetics, and mechanical strength, are dependent on both the incorporated peptides, as well as their sequence within the chain [88,89]. Further, the mechanical properties of a peptide-based hydrogel can be tailored through varying the assembly conditions including peptide concentration, charge, pH, and temperature among others [89]. Generally, peptide-based hydrogels can be functionalized through addition of bio-functional motifs, degradable sequences, therapeutic components, or growth factors on side chains or terminal sites [89]. For example, addition of matrix metalloproteinase (MMP) and MMP cleavable sequences, has been utilized to tune degradation properties of peptides, as MMPs are naturally occurring enzymes capable of degrading structural ECM components [89]. Short chain peptides (<21 peptide linkages) are cost effective and tend to be easier to synthesize in comparison to longer chain peptides; however, they often lack mechanical strength [88,90]. Dipeptide hydrogels require the presence of additional aromatic groups within their structure to support gel formation and mechanical strength during self-assembly [88]. The printability and mechanical stability of modified 9-fluorenylmethoxycarbonyl (Fmoc) dipeptides have been improved through layering the dipeptides with oppositely charged terminal residues to promote electrostatic interactions, forming a stable structure without additional cross-linking [90]. Other approaches to increase mechanical stability for 3D bioprinting include modifying elastin-like poly-peptides to be photosensitive [91]. Multi-domain peptides have been further studies for determination of how their chemical functionality affects the host response, and it was found that negatively charged peptides elicited minimal inflammatory response with fast remodeling, while positively charged peptides triggered immune infiltration, promotion of angiogenesis and collagen deposition [92]. Although peptide-based hydrogels are highly promising for application in 3D bioprinting, they still face technical challenges including methods of sterilization, batch-to-batch reproducibility, and large-scale production [89].

2.1.2. Synthetic polymers

While generally incompatible with direct cell incorporation, synthetic polymers play a very important role in extrusion-based bioprinting techniques for enhancing the mechanical properties of printed structures. Although bioinks are generally not formed directly from synthetic polymers due to the process conditions required for their printing (elevated temperatures, organic solvents etc.) [93], these polymers are commonly used or printed to form a scaffold framework with strong mechanical strength; and then cell-incorporating hydrogels are bioprinted or impregnated into the space of the frameworks, forming hybrid scaffolds [364]. The synthetic polymers commonly employed in 3D extrusion bioprinting techniques are outlined below.

Poly(ε-caprolactone) (PCL) is a polyester that can be degraded by hydrolysis in physiological conditions (such as in human body fluids) and therefore has drawn considerable attention for use as an implantable biomaterial [94]. PCL has a low melting point (60 °C), is hydrophobic, and degrades slowly making it favorable for numerous applications in tissue engineering (e.g., drug delivery, anti-adhesion barrier films, bone substitutions) [94]. PCL has been utilized in 3D-printing due to its thermoplastic behavior, respectable mechanical strength, and hydrolysis-induced biodegradation profile. In its liquid phase, PCL is thermally stable and demonstrates flow behavior appropriate for printing [94]. When printed onto a low-temperature printing stage, PCL can quickly solidify and form mechanically-stable 3D constructs with good structural fidelity [6,94]. Notably, the melting temperature of PCL is too high to sustain cell viability; therefore, printed PCL scaffolds require cell seeding after scaffold fabrication, impregnation, or printing with another hydrogel bioink with cells to form a hybrid scaffold structure [35–38,95–97]. Generally, the combination of PCL with other biocompatible polymers broadens its application to tissue engineering including guided bone regeneration membranes, surgical sutures, drug-delivery capsules, etc. [98–100]. Coupling PCL with polyethylene glycol (PEG) causes amphiphilic thermosensitive behavior meaning the mixture is able to undergo rapid and reversible physical gelation by controlling the temperature [97]. PCL is commonly used in bone tissue engineering due to its ease of manipulation, biocompatibility, stability, and U.S. Food and Drug Administration (FDA) approval for use in some products [35,39,94,101]. Due to the hydrophobic and non-osteogenic nature of PCL, incorporation of active bioceramics, such as hydroxyapatite, is considered as an effective approach to improve the mechanical properties, cell attachment and hydrophilicity [35,40,86,94,102,103].

Poly(ethylene)-based polymers (mainly poly(ethylene glycol) (PEG) and poly(ethylene oxide) (PEO)) are the most widely used synthetic hydrogels in scaffold bioprinting for tissue engineering applications, primarily due to their tailorable properties [104]. They are produced by the polymerization of ethylene oxide by condensation and can be classified as PEG or PEO based on molecular weight. PEG and PEO are able to bind water molecules, thereby increasing intraluminal water retention. PEG and PEO, which can be dissolved in water, are metabolically inert and biocompatible which reduces the immunogenicity after implantation [105]. The solutions can be crosslinked into hydrogels via physical, ionic, or covalent bonding methods. PEG and PEO hydrogels possess high permeability, facilitating the exchange of nutrients and waste materials to support cell metabolism; therefore, they are often adopted to encapsulate cells for cell delivery [106,107]. However, these hydrogels provide limited support for protein binding and cell adhesion due to their synthetic nature. To overcome this limitation, PEG/PEO hydrogels are often modified with peptides, such as RGD peptide, that have the capacity to enhance cell adhesion [108]. For scaffold bio-printing, PEG/PEO solutions are often tailored to be photopolymerizable using either acrylates or methacrylates [106,107]. These modified solutions can be efficiently crosslinked by UV light to achieve improved mechanical stability after extrusion. PEG hydrogels can be utilized as scaffold materials for cell encapsulation, and as vehicles for vaccine delivery systems [109–111]. Copolymerization with other synthetic polymers, such as poly vinyl alcohol (PVA), can also be

used to alter the degradation PEG hydrogels [104].

Pluronic® is a tri-block copolymer based on poly(ethylene oxide) (PEO) and hydrophobic poly(propylene oxide) (PPO), arranged in an A-B-A triblock structure (PEO-PPO-PEO) [112]. It is thermosensitive as PPO side chains become less soluble above a threshold temperature between 22 and 37 °C (depending on polymer concentration) and gelation occurs. Pluronics have surfactant properties that enable them to interact with hydrophobic surfaces and biological membranes due to their amphiphilic characteristics (presence of hydrophobic and hydrophilic components) [113]. However, owing to its synthetic nature, Pluronic has disadvantages including limited cell adhesion and degradation [114]. Previous research also shows it dissolves significantly after one week of culture and has questionable cytocompatibility due to potential disruption of the cell membrane [114,115]. Pluronic can be used as a sacrificial bioink for use in making molds, channels, vessels, or vasculature for 3D bioprinting or as a temporary support structure [116]. Nonetheless, the advantages of Pluronic, such as high viscosity and good printability, still make it attractive for bioprinting constructs with good shape fidelity [111].

2.1.3. Composite polymers

The use of composite biomaterials allows for synergistic properties and performance. The biocompatibility of natural polymers and mechanical properties of synthetic polymers make both classes of polymers attractive materials for tissue engineering. However, the mechanical/biological properties of a single material are often limited, raising the need for composite materials. Additionally, the properties of a single material may not always be easily controlled or consistent, thus degrading its suitability for certain applications [117]. Generally, there are two types of hydrogel composites made from: 1) two or more hydrogel-forming polymers and 2) polymer(s) with fillers for reinforced or enhanced properties.

Hydrogel-forming polymers can be combined with two or more natural and/or synthetic polymers with synergistic properties. Composite hydrogels were synthesized form collagen type I and ECM protein with improved mechanical and biological properties as compared to gels obtained from one material alone [118]; and also from alginate and collagen type I with improved rheological and indentation properties [119]. In the context of bioprinting, a number of composites have been synthesized from dECM/alginate [33], alginate-hyaluronic acid [63], alginate dialdehyde-gelatin [42,43], chitosan-alginate-hydroxyapatite [17], alginate-carboxymethyl chitosan [46], and alginate-gelatin [120] among many others.

For the composite hydrogel(s) with fillers, the most widely used fillers are inorganic ceramic-like hydroxyapatite and carbon-based materials such as graphene. Inspired by the naturally occurring bioactive nanomaterials found in biological systems, researchers are developing novel bioactive biomaterials by combining inorganic ceramics with natural or synthetic polymers for enhanced mechanical/biological properties, as well as printability in the context of bioprinting. A wide range of bioactive ceramic nanoparticles, including hydroxyapatite, silicate nanoparticles, and calcium phosphate, have been applied to synthesize composite hydrogels [40,94,121]. Carbon-based materials can also be introduced to enhance conductivity in biomedical engineering applications [122], and properties and functions of bioprinted or engineered scaffolds [123,124]. Indeed, a number of composite materials with fillers have been developed for bioprinting, with improved printability, electroactivity, and biocompatibility [125–128].

2.2. Preparation of biomaterial solutions and bioinks

For bioprinting, biomaterials or polymers are available in the forms of gels, powders, and/or particles, and have to be prepared in solution form by using water or other solvents. Polymers are either water soluble or non-water-soluble. A water-soluble material can be directly dissolved into water or water-based solutions. Widely used biomaterials for printing, such as alginate and gelatin, are water-soluble materials and can take minutes to hours to dissolve. Many materials dissolve slightly in water under conditions of neutral pH and room temperature but can be easily dissolved at non-neutral pH or elevated temperature. These materials, such as chitosan, collagen, and polyvinyl alcohol (PVA), are also classified as water-soluble materials. Non-water-soluble biomaterials that are utilized in extrusion-based bioprinting for scaffold fabrication must be processed into solution-like phases before application. To achieve this, these non-soluble materials are either dissolved in special organic solvents (e.g., chloroform for polycaprolactone (PCL)) or thermally melted by controlling the temperature during material extrusion. Table 1 summarizes common biomaterials used in scaffold bioprinting, along with gelation or crosslinked methods (more discussed in Section 3.3).

To fabricate constructs for mimicking native tissues/organs, biomaterial solutions may need to be prepared with living cells (to form bioinks) for bioprinting. As such, the prepared solutions must provide an aqueous environment that is both favorable for cell survival and suitable for printing. Currently, the most widely used biomaterials for cell bioprinting are polymers or gelled polymers or hydrogels, which can provide a mild environment to ensure the vitality of mixed cells in the solutions, while the hydrogel formed after solidification contains a large amount of water and possesses similar properties to natural tissues. Natural hydrogels are popular due to their inherent biocompatibility, while synthetic hydrogels have more uniform and predictable properties. The most commonly used hydrogels include alginate, chitosan, agarose, hyaluronic acid (HA), collagen, gelatin, fibrin, poly(ethylene glycol) (PEG), and poly(ethylene oxide) (PEO). decellularized matrix (dECM) components have also been developed as biomaterials for scaffold bioprinting with cells (Table 1).

Notably, one major challenge when creating constructs from natural hydrogels is their limited mechanical properties. To address this challenge, some non-water soluble polymers with high mechanical strength are often used in extrusion bioprinting in combination with hydrogels to develop hybrid scaffolds [2,6]. These materials are normally dissolved in solvent or melted inside the bioprinter by temperature control during the printing process, then extruded in a layer-by-layer pattern to form scaffold frameworks. Because the solvent used or elevated temperature environment can lead to serious problems with respect to cell and tissue survival, cells cannot be added to or mixed in these materials. The most extensively used of such materials in extrusion bioprinting are polycaprolactone (PCL), polylactic acid (PLA), polyglycolic acid (PGA), and their copolymers [101].

3. Important properties bioinks for bioprinting

During the extrusion bioprinting process, the bioink is loaded into the printer cartridge and then extruded to form 3D constructs with the help of suitable crosslinking reactions or mechanisms. Successful bioprinting of constructs and their successful use in subsequent applications relies on the properties of the formulated bioinks, including physical, rheological, crosslinking, mechanical, and biological properties.

3.1. Physical properties

The surface tension and wettability of a bioink are of important physical parameters for extrusion bioprinting. The surface tension of a bioink is the internal force exerted on a unit length contour bounding the bioink surface and plays a critical role in the formation of bioink filaments once printed. On one hand, a large surface tension causes the formation of droplets or attachment to the nozzle tip during printing; on the other hand, once deposited on the platform, the large surface tension can help retain the filament shape or profile. The wettability of a bioink is the ability to maintain contact (at a certain contact angle) with solid surfaces including the nozzle and print bed. It is an important parameter affecting the first layer of bioink deposited on the printing stage. Fig. 3

Table 1
Common biomaterials and their solution preparation/gelation methods, along with their merits/demerits and applications.

Biomaterials	Water soluble or non-soluble	Typical preparation conditions	Gelation or crosslinked methods	Merits	Demerits	Applications	References
Alginate	Water soluble	Dissolves within hours in water or water-based solutions at room temperature [41,129]	Ionic and pH crosslinking [22,32,41,130–132]	• Low price • Easy to fabricate 3D structures • Good biocompatibility • Easy gelation • High biodegradability and low immunological stimulation • Retains cell viability and osmolar requirements of cells • A suitable material for 3D printing due to crosslinkable features • Shear-thinning behavior	• Bioinert • Limited long-term stability • Rapid loss of mechanical properties during in-vitro culture • Limited 3D shape-ability • Low degradation	• Bone • Cartilage • Cardiovascular • Liver • Muscle • Nerve • Wound • Drug delivery	[133–142]
Chitosan	Water soluble	Dissolves within hours in weak acid at room temperature [47]	Thermal crosslinking [143]	• Ingredients resemble ECM components of native tissue • Non-toxic by-products • Induces cell adhesion proliferation, differentiation, and viability • Antimicrobial • Partially osteoconductive	• Slow gelation rate • Poor mechanical properties • Can conflict with printing of cells and pH-sensitive molecules • Slow gelation	• Drug delivery and gene therapy • Bone • Skin • Bioadhesives • Cartilage • Blood vessels • Neural • Cornea	[144–149]
Agarose	Water soluble	Easily dissolves in near-boiling water or water-based solutions [150]	Thermal and chemical crosslinking [151]	• Responsive to temperature • Rapid gelation • Gelation at physiological temperature • Mechanically robust	• Poor cell attachment • Excessive water uptake	• Cartilage • Bone • Targeted drug delivery • Spinal cord • Pancreas • Skin • Wound • Neural • Cardiac	[152–159]
Hyaluronic acid (HA)	Water soluble	Dissolves within hours in weak acid at room temperature [160,161]	Physical crosslinking (controlling pH, temperature and ions) and chemical crosslinking [162]	• Good biocompatibility • Non-toxic degradation by-products • Visco-elastic properties • Highly hydrophilic • Anti-microbial properties • Good shear thinning properties	• Poor mechanical strength • Fast degradation rate • Required modification for stable cross-linking	• Cartilage • Drug and gene delivery • Wound healing • Odontology • Wound treatment • Ophthalmology • Urethra	[158,163–169]
Collagen	Water soluble	Dissolves in weak acid at room temperature and gels at neutral pH at 37 °C [170]	Photo crosslinking [171]	• Low immunogenicity • Good biocompatibility • Biodegradability • Regulates cell adhesion and differentiation	• Poor mechanical properties • Loses shape and consistency • Low viscosity and slow gelation	• Spinal repair • Vascular • Dental • Cartilage • Bone • Corneal • Oral mucosa • Wound healing • Heart tissue repair	[172–176]
Gelatin	Water soluble	Dissolves in water or water-based solutions at $\geq$ 40 °C and gradually gels as temperature drops [177]	Physical, chemical, and enzymatic	• Derivative of collagen • Accelerates gelation time	• Poor mechanical properties • High degradation rate	• Cartilage • Wound healing • Heart tissue repair • Cornea	[180–184]

(continued on next page)

Table 1 (*continued*)

Biomaterials	Water soluble or non-soluble	Typical preparation conditions	Gelation or crosslinked methods	Merits	Demerits	Applications	References
			crosslinking [178]	• Capable of reversible thermal gelation • Biocompatible • Biodegradable		• Neovascularization • Bone • Muscle • Ligament [179] • Drug delivery	
Fibrin	Water soluble	Dissolves within minutes in water or water-based solutions at room temperature [185]	Enzymatic crosslinking [186]	• ECM functional protein • Highly bioactive • High cell adhesion	• Rapid degradation • Poor mechanical properties	• Wound healing • Drug and growth factor delivery • Regeneration of stem cells, bone, peripheral nerves, and other injured tissues • Hemostasis	[78, 187–191]
Poly(ethylene glycol) (PEG)	Water soluble	Dissolves in water or water-based solutions at room temperature and polar solvents such as acetone [192]	Physical crosslinking [193]	• Chemically well-defined • Allows for versatile chemical modifications • Highly water-soluble • High capacity for chemical modification	• Poor biodegradability • Poor cell attachment	• Wound healing • Drug delivery • Bone • Cartilage	[194–199]
Poly(ethylene oxide) (PEO)	Water soluble	Dissolves in water or water-based solutions at room temperature and polar solvents such as acetone [200]	Physical crosslinking [201]	• Hydrophilic • biocompatible and biodegradable • non-immunogenic	• Lack of cell specific adhesion • Poor mechanical properties for hard tissue engineering	• Wound healing • Bone	[202–206]
Polyvinyl alcohol (PVA)	Water soluble	Dissolves within minutes in water or water-based solutions over 40 °C [207]	Chemical and physical crosslinking [208,209]	• Good biocompatibility • Suitable mechanical strength • Highly hydrophilic	• Inability to support cell attachment • Fast degradation	• Bone • Cartilage • Wound dressing • Vascular grafts • Nervous • Corneal • Kidney • Artificial meniscus • Artificial Pancreas	[210–215]
Decellularized matrix (dECM)	Water soluble	Dissolves in acetic solutions in low temperature [84]	Chemical and physical crosslinking [84]	• Great biocompatibility • Support cell growth and viability • Source of bioactive molecules •	• Poor mechanical properties • Hard to print without modification	• Skin • Bone • Nerve • Heart • Lung • Liver • Kidney • Urethra • Corneal • Muscle	[83,84, 213]
Polycaprolactone (PCL)	Non-soluble	Dissolves in organic solvent such as chloroform; melts at 60 °C [216,217]	Physical crosslinking [94]	• Low cost • Tunable degradation • Excellent rheological and viscoelastic properties upon heating • high mechanical toughness at physiological temperature	• Hard tissue engineering • Long-term degradation • Lack of biofunctional groups • Adheres poorly to cells	• Bone • Cartilage • Wound healing • Heart	[218–224]
Polylactic acid (PLA)	Non-soluble	Dissolves in organic solvents such as propanol; melts at 170 °C [225,226]	Physical crosslinking [227]	• Biocompatible • Controllable degradation rates in vivo • High elastic modulus	• Low cell adhesion • Biological inertness • Low degradation rate • Acid degradation by-products	• Bladder • Cartilage • Liver • Adipose • Bone • drug encapsulation and delivery systems • Wound healing • Vascular grafts •	[228–233]
Polyglycolic acid (PGA)	Non-soluble	Dissolves in solvents such as hexafluoroisopropanol; melts at 225 °C [234,235]	Physical crosslinking [236,237]	• Biodegradable • Biocompatible • High strength	• Fast degradation • Expensive	• Drug delivery career • Bone • Cartilage • Tooth	[238–242]

(*continued on next page*)

Table 1 (*continued*)

Biomaterials	Water soluble or non-soluble	Typical preparation conditions	Gelation or crosslinked methods	Merits	Demerits	Applications	References
				• Tunable mechanical properties • Erosion resistant • Hydrophil • Possibly antibacterial		• Tendon • Spinal regeneration	

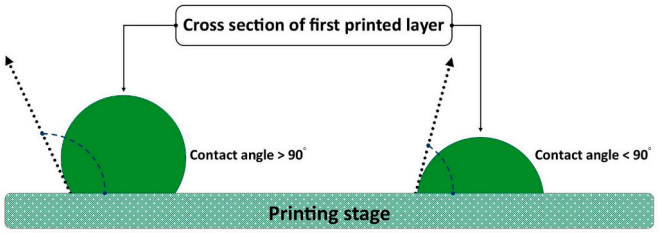

Fig. 3. The first layer formed in the bioprinting process.

shows two strands formed with different contact angles (the angle between the printed strand profile and the printing stage). A large contact angle helps maintain the fidelity of the printed hydrogel structure in the vertical dimension, while a small contact angle helps anchor the printed construct on the printing stage and avoid undesired movement and possible deformation during the layer-by-layer printing process, thus helping maintain the structural integrity [39,41,63].

3.2. Rheological properties

The rheological or flow behavior of a bioink, associated with its resistance to flow, is typically characterized by the relationship between the shear stress and shear rate within the bioink, where the ratio of shear stress to shear rate is termed as the apparent viscosity or simply viscosity. Bioink flow behavior can be regulated by biomaterial concentration, cell density, temperature, as well as the methods to synthesize the bioink or biomaterial solutions [31,34,94,243–245], with an example of experimental results of an alginate-based bioink illustrated in Fig. 4.

To characterize the flow behavior of a biomaterial solution, there are various models available for this purpose. Commonly used models are of the power-law model, generalized power-law model, Carreau fluid model, Ellis fluid model, and Casson fluid model [3]; and among them the generalized power law equation (also called three-parameter Herschel-Bulkley model) has been widely used in the literature [31,246], which is given:

$$\tau = \tau_0 + K\dot{\gamma}^n \quad (1)$$

where t and t_0 are the shear stress and the yield stress, respectively; the fluid exhibits solid properties when $t < t_0$, and for $t > t_0$ exhibits shear thinning when $n < 1$ and shear thickening when $n > 1$. $\dot{\gamma}$ is the shear rate; K is the consistency index with a unit of Pa $\times$ s^n; and n is the flow behavior index (dimensionless). For Newtonian behavior, $t_0 = 0$ and $n = 1$. Physically, K is a measurement of viscosity (i.e., higher K for more viscous fluids) and n is a measure of the degree of non-Newtonian behavior (i.e., non-Newtonian behavior becomes more pronounced as n departs from unity). For a given fluid, the values of n, t_0, and K are identified and determined from the measured flow behavior. Typically, n is identified as a constant while t_0 and K are functions of concentration and temperature to account for their influence on the flow behavior [31,247]. To experimentally measure and characterize the flow behavior of biomaterial solutions or bioinks, the commonly used techniques and/or equipment, including capillary rheometers, cone-and-plate rheometers, parallel plate rheometers, and oscillatory rheometers, as described in Ref. [2].

Bioink flow behavior can significantly impact the bioprinting process. On the one hand, higher viscosity can enhance the printability (as discussed in Section 5) because a more viscous bioink, once printed, is more difficult to flow and spread, thus helping maintain the printed filament and 3D structure. Also, bioinks with sufficient viscosity can retain the encapsulated cells in position and can prevent inhomogeneous cell distribution or sedimentation. On the other hand, higher viscosity needs a larger pressure for bioprinting, increasing the process-induced forces on the cells and thus degrading the cell viability (as discussed in Section 5). Shear-thinning behavior (where viscosity decreases with the flow rate) is often desired in bioprinting due to the facts that during the printing process, the bioinks become less viscous as the shear rate increases. As the shear stress is removed after exiting the printing needle or nozzle, the bioink viscosity rapidly recovers, leading to high filament fidelity. For characterizing the shear thinning properties of bioinks, the above generalized power law model has been widely used, where the shear thinning behavior is represented by the power law index with a value less than 1 (smaller value, more profound shear thinning behavior) [2].

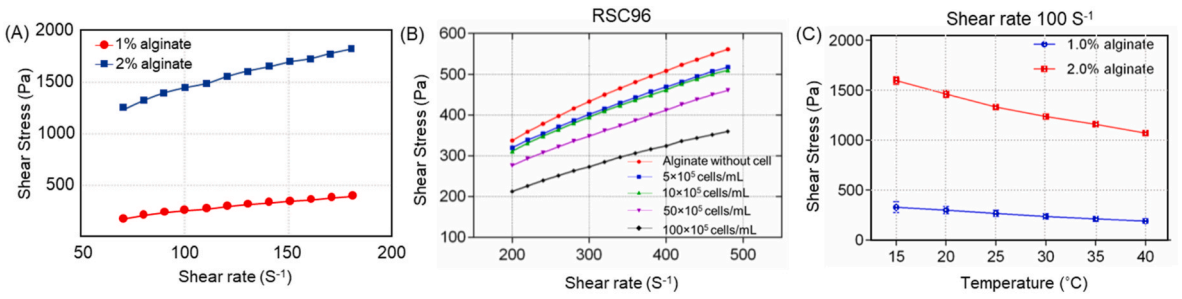

Fig. 4. Flow behavior of alginate-based bioink changing with alginate concentration (a), cell density (b), and temperature (c) [34].

3.3. Crosslinking mechanism

An important step in the bioprinting process is the transition from a biomaterial solution or bioink to a gelled or crosslinked hydrogel. By the crosslinking process, polymer chains are joined together by either physical methods and/or chemical reactions, thus producing a hydrogel with a structurally stable polymeric network. While a variety of methods have been available [248], the common ones employed in bioprinting mainly include ionic, thermal, photo, and enzyme crosslinking.

Ionic crosslinking occurs when a water-soluble and charged polymer crosslinks with ions of opposite charge. Alginate, for example, is a well-known example of a polymer that can be crosslinked by divalent metal ions, such as Ca^{2+}, Ba^{2+}, and Zn^{2+} [30]. Ionic crosslinking is an important mechanism in bioprinting as it provides mild and instant gelation of the polymer solution. Its drawbacks include limited mechanical strength, as well as the release of metal ions into the body after implantation. For ionic crosslinking, water-soluble calcium salts such as calcium chloride ($CaCl_2$), calcium sulfate ($CaSO_4$), and calcium carbonate ($CaCO_3$) are commonly used for crosslinking. Addition of Ca^{2+} ions (or other di/trivalent cations) causes rapid gelation of the solution. Because this crosslinking happens instantaneously under physiological conditions, ionically crosslinked hydrogel have been widely employed in bioprinting for tissue engineering applications [32,130]. **Thermal crosslinking** occurs in polymers that are sensitive to temperature, where increasing or decreasing temperature can lead to crosslinking or gelation. Polymers forming hydrogels through thermal crosslinking, such as agarose, gelatin, and collagen, have a gel transition temperature below which the solution gels. Typically, gels formed by thermal crosslinking are mechanically weak. **Photo crosslinking** refers to the photo-induced formation of a covalent bond between macromolecules to form a crosslinked network. Photo-curable polymers can be printed to form 3D hydrogels if illuminated by a laser or visible light. Some other polymers, such as proteinaceous biopolymers, which contains tyrosine residues (such as collagen, fibrin, and gelatin), can be photo-crosslinked only if an appropriate photoinitiator is incorporated [249]. Although many polymers cannot be directly crosslinked by light, a chemical reaction with an acrylate or methacrylate-based agents makes them photo-crosslinkable. These polymers are usually crosslinked by UV light, typically, with wavelengths in the 320–365 nm range. Notably, the use of UV light has potential biological risks as the UV light may damage cells in the printed constructs and may also be harmful to the operators. Photo crosslinkable polymer bioprinting has been reported by using gelatin-methacrylate, hyaluronan-methacrylate, and dextran-methacrylate [124]. **Enzyme crosslinking** utilizes enzymes as catalysts to form the covalent bonds between protein-based polymers. This method is promising for use in bioprinting due to the mildness of the enzymatic reactions for preserving the cell viability. In bioprinting, several enzymes have been used, including microbial transglutaminase [250], tyrosinase (Ty) [251], and horseradish peroxidase (HRP) [252,253]. Enzyme crosslinking has been commonly employed for forming hydrogels from HA, gelatin, fibrinogen, polypeptides (PLys-*b*-(-PHIS-*co*-PBLG)-PLys-*b*-(PHIS-*co*-PBIG)-*b*-Plys), and chitosan [254]. The limitations of enzyme crosslinking include the difficulty in obtaining the enzymes, limited mechanical properties of the hydrogels produced, and less active property in the culture media or scaffolds [255,256]. In addition, enzyme-catalyzed crosslinking may be sensitive to environmental conditions such as temperature and pH, thus affecting and degrading the crosslinking or bioprinting process.

3.4. Mechanical properties

The mechanical properties of biomaterial or bioink hydrogels play an important role in tissue engineering applications. The constructs printed from biomaterials or bioinks are typically incubated in bioreactors (in vitro) for maturation, and subsequently implanted within living bodies (in vivo) where they provide cells with a 3D structure and mechanical support for cellular processes such as migration, proliferation, and/or differentiation, resulting in the growth of a functional tissue-engineered construct or viable tissue. The mechanical properties of bioinks or printed constructs are featured by their mechanical strength and degradation. As such, the mechanical properties of constructs are dynamic, with the decrease in biomaterial strength caused by degradation being combatted by an increase in mechanical strength due to tissue regeneration. Eventually, the mechanical properties of the construct should be similar to those of the tissue/organ being repaired throughout regeneration. It is generally accepted that the mechanical properties of a construct at the initial stage of implantation or of a combined construct of scaffold biomaterials and regenerated tissue during the healing process should be similar to that of the tissue/organ being repaired [257–259].

In many tissue engineering applications, elasticity and stiffness are of important mechanical properties [260–262]. These mechanical properties are typically characterized by the relationship between an applied force and the resulting deformation. For characterization, loading conditions commonly applied to specimens during mechanical testing are tensile/compressive forces, bending moments, and torque; with the deformation caused by these forces measured to obtain stress-strain curves. From these curves, the elastic moduli and yield stresses are typically characterized by bioprinted materials and/or constructs [2,263]. The selection of loading conditions depends on the intended applications or biomechanical conditions of the tissue/organ being repaired, as well as the biomaterials or hydrogels used. For example,

Table 2
Mechanical properties and characterization methods for various hydrogels.

Hydrogel	Mechanical characterization method	Properties determined	Reference
Alginate	Compression test	Compressive modulus and strength	[265,266]
Chitosan	Tensile and compression test	Tensile and compressive strength	[267]
Gelatin	Rheological and tensile test	Loss and storage modulus, tensile strength	[268]
Agarose	Rheological, compression and tensile test	Loss and storage modulus, tensile and compressive strength	[269,270]
Collagen	Rheological and tensile test	Loss and storage modulus, tensile strength, ultimate strain, resilience, toughness	[271,272]
Poly(ethylene glycol)	Rheological and confined compression test	Loss and storage modulus, loss tangent, elastic modulus	[273]
Poly(ethylene oxide)	Tensile test	Elastic modulus, tensile strength	[274]
Poly vinyl alcohol	Tensile test	Percentage elongation, elastic modulus, tensile strength, toughness	[275,276]
PCL	Tensile test	Tensile and yield strength, elastic modulus, percentage elongation	[277,278]
Polylactic acid	Tensile, bending, shear and impact test	Yield strength, elastic modulus, percentage elongation, flexural strength and modulus, shear strength, impact strength	[279,280]

compression testing is often used in bone/cartilage tissue engineering [15,16,263,264], whereas tensile testing is often used in tendon/lung/heart tissue engineering [11,14,28,227,378]. Also, the selection of loading conditions. Table 2 outlines the testing methods and the mechanical properties of common hydrogels used in tissue engineering applications.

Given that many of soft or stiffer tissues, such as nerves, skin, lung, bone, and tendon, exhibit complex time and rate dependent mechanical properties [281–283], recent studies also started to look at the viscoelastic characterization for tissue engineering applications. Having both fluid and elastic properties, a material or bioink hydrogel may exhibit both viscous and elastic characteristics when undergoing deformation. For this, viscoelasticity is typically characterized in terms of storage modulus and loss modulus. The storage modulus presents the ability of a viscoelastic material to store energy in an elastic manner, while the loss modulus represents the energy dissipated in the viscous component of the material. Notably, for a given material or solution, the storage modulus and loss modulus, as characterized by, for example, an oscillatory rheometer, are typically not constant, but depend on the frequency and amplitude of the sinusoidal stain applied. For such cases, frequency sweep tests (e.g., from 0.01 to 100 Hz at a constant strain) and strain sweep tests (e.g., from 0.01 to 100% at a constant frequency of 1 Hz) are performed to measure and characterize the storage modulus and loss modulus, as well as the loss angle (or the phase angle between the stress and strain), as shown in Fig. 5 [43]. The mechanical properties of a viscoelastic biomaterial can also be quantified with the help of creep and relaxation tests [284]. The creep test is performed to analyze the behavior of the material under a constant applied load or stress, whereas stress relaxation test is performed under a constant deformation or strain.

3.5. Biological properties

Biological properties of materials for bioprinting are typically characterized by their biocompatibility, biodegradation, and immunogenicity. Biocompatibility refers to the ability to support cell growth/functions, such as cell survival, attachment, proliferation, differentiation, and tissue regeneration [1–3]. In the bioprinting process, living cells are mixed with the hydrogel-forming polymer solution to form a bioink and then go through the bioprinting process. During bioprinting,

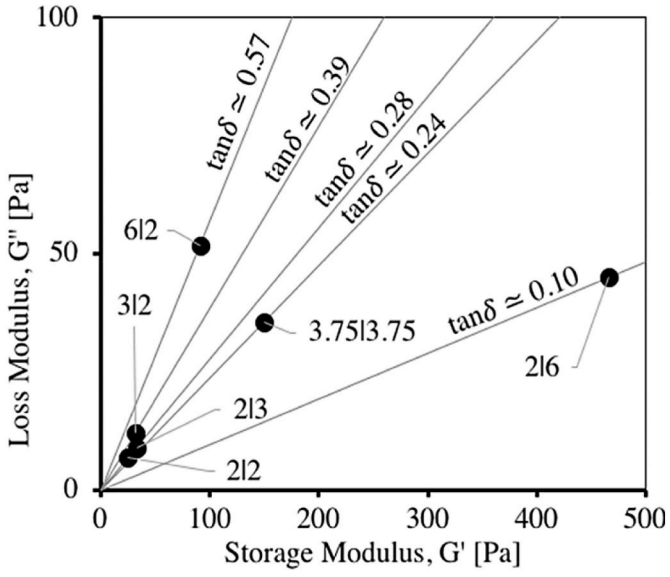

Fig. 5. Measured storage modulus and loss modulus, along with the loss angle, of alginate dialdehyde (ADA) – gelatin (Gel) hydrogels of varying concentrations (or the ratio of ADA:Gel as 6:2, 3:2, 2:2, 2:3, 2:6, and 3.75:3.75) [43].

cells are exposed to process-induced harsh conditions, such as shear stress and/or elevated temperatures, which may cause cell damage. As a result, only some cells in the bioink survive the bioprinting process. Cell viability refers to the percentage of live cells post-printing to the total number of cells incorporated [285]. Cell viability assays are used to measure and determine the proportion of healthy cells within samples, and various assays have been adopted to examine the cell viability within printed constructs. To distinguish damaged cells from normal cells, dyes such as azo dye trypan blue or fluorescent dyes calcein-AM and propidium iodide have been widely used due to their ability to selectively stain live and dead or damaged cells [2]. Notably, cell viability of extrusion bioprinting varies widely, depending on the cell type [5,43,286–291]. After bioinks have been printed, the formed constructs play an important role in supporting cell viability, as well as other cell functions through cell attachment, proliferation, differentiation, and/or tissue regeneration.

Materials for printing or bioprinting should degrade to monomers that are water-soluble, nontoxic, and can be metabolized by the liver and/or excreted via the kidney. Also, the degradation mechanisms and by-products obtained should not elicit harmful changes that cause damage to the regenerating tissue and/or surrounding tissues. Hydrogels formed in bioprinting can be degraded by water-induced cleavage of certain bonds/chains (or hydrolysis) in an aqueous environment and/or by enzymatically-induced cleavage with the presence of specific enzymes. Biodegradation through hydrolysis usually occurs via bulk and/or surface degradation mechanisms, while in enzymatic degradation, the bond/chain cleavage in the hydrogel is caused by the catalytic action of enzymes under abiotic conditions, with the rate dependent on both the number of cleavage sites and the enzyme concentration. For a given hydrogel, the degradation rate can be affected or regulated by several factors. The cell/polymer ratio is one of them, where cells are the source of matrix remodeling proteases, and thus relatively lower cell densities or higher polymer concentrations can decrease the degradation rate, thus extending degradation time; however, lowering the cell density can also lead to poor tissue regeneration [1–3]. Another way to adjust the hydrogel degradation time is controlling the degree of crosslinking within the polymeric network. Increasing the polymer concentration, crosslinking agent concentration, and exposure time of the crosslinking agent are methods to achieve higher crosslinking and thus slower degradation rates [32,151,162,251]. Researchers have also modified the hydrogel-forming polymers with peptides that are sensitive to enzymatic degradation to achieve control over the degradation behavior of hydrogels [253,255]. The degradation behavior of hydrogels is mainly determined by calculating weight changes with respect to their initial condition.

Immunogenicity of a biomaterial or bioink is its capacity to provoke an immune response upon its implantation in vivo. The biomaterials and cells in printed constructs are both potential antigenic sources that may cause the innate immune system to respond to form a fibrotic capsule to isolate the implanted material, or the acquired immune system to respond causing an antigen-specific reaction. Naturally derived biomaterials are susceptible to acquired immunity owing to the presence of antigens, while synthetic biomaterials are usually susceptible to innate immunity [1–3]. The immunogenicity of a biomaterial is important because an intense immune response can lead to shorter scaffold degradation times, a potential attack on the embedded cells, and a higher possibility of fibrosis rather than tissue regeneration.

4. Extrusion bioprinting of constructs

Extrusion bioprinting systems are configured to deposit or print continuous strands or fibers of bioinks to form 3D structures layer-by-layer. An extrusion-based bioprinting system typically resembles the configuration schematically shown in Fig. 6, which consists of a printing head, a three-axis positioning system, and a printing stage, all controlled by a computer. The positioning system is used to move the printing head

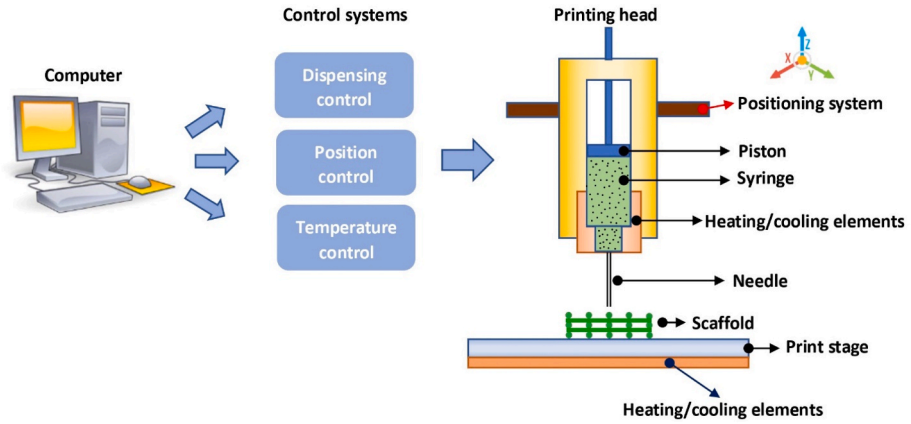

Fig. 6. Schematic of a typical extrusion-based bioprinting system.

relative to the printing stage in the *X, Y,* and *Z* directions, while the printing head deposits the bioink that is loaded in the syringe onto the printing stage. Temperature control is used to regulate the temperature of both the bioink and printing stage, typically in a range from 10 to 200 °C. The bioink loaded in the syringe is driven through the needle, which typically has either a cylindrical or tapered shape with a diameter ranging from 0.1 mm (or 100 μm) to 2 mm. The printed strand diameter and resolution are largely determined by the needle diameter, with higher resolution strands achievable by means of smaller needles. For bioprinting constructs, the flow rate of the biomaterial, design and corresponding structure formed, process-induced forces, and cross-linking of biomaterial solutions are all critical.

4.1. Flow rate in extrusion printing

During bioprinting, bioinks are printed to form constructs with a 3D structure by stacking the printed strands layer-by-layer and, as such, the characteristics of the printed strands affect the structure of the printed scaffold. The size of the printed strands is proportional to the flow rate of the bioink printed, i.e., the volume (or mass) of the bioink forced out of the needle per unit time. The flow rate can be affected by such factors as the process parameters (e.g., printing forces and temperature), structural parameters (e.g., needle geometry and size), and bioink flow behavior. One way to represent the flow rate in bioprinting is to develop empirical models from experimental data, but this typically requires exhaustive and time-consuming experiments. A more efficient way to represent the flow rate of the bioink being printed is based on physical laws, resulting in analytical models that form a basis to rigorously regulate the flow rate in the bioprinting process [31,246,291,292].

For pneumatic-driven bioprinting, pressurized air is used to drive the bioink in the syringe through the needle. For bioinks or biomaterial solutions with flow behavior described by the generalized power law, i.e., Equation (1), the flow rate is given by [293].

$$Q = \frac{\pi D^3}{8K^{1/n}\tau_w^3}(\tau_w - \tau_0)^{(n+1)/n} \times \left[\frac{n}{3n+1}\tau_w^2 + \frac{2n^2}{(2n+1)(3n+1)}\tau_w\tau_0 + \frac{2n^3}{(n+1)(2n+1)(3n+1)}\tau_0^2\right] \quad (2)$$

where τ_w is the shear stress at the needle wall and given by

$$\tau_w = \frac{R\Delta P}{2L} \quad (3)$$

The above equations illustrate that the flow rate of the bioink depends on its flow behavior (via τ_0, K, and n), can be regulated by changing the printing process parameters (via ΔP), and is affected by the structural parameters of the needle (via R and L). If the bioink flow behavior and parameter values are known, one can calculate the flow rate of the bioink during the printing process. These equations also provide a means to determine the printing pressure required for a given needle to achieve the desired flow rate for scaffold fabrication. In pneumatic-driven bioprinting, needle geometry is another factor affecting the bioink flow rate; under the same printing pressure, the flow rate using a tapered needle is much higher than when using a cylindrical needle [291]. Associated with the flow rate, extrudability in bioprinting refers to the capability to extrude or print the bioink through a needle to form a continuous and controllable filament [285].

Both screw-driven and piston-driven systems allow for more direct control over the flow rate of the bioink compared to pneumatic-driven systems. It has been shown that the flow rate in screw-driven systems involves two components [5,6]. One component is the rate of drag flow due to the screw rotation, proportional to the screw speed and the other component is the rate of pressure-driven flow, proportional to the pressure drop. As such, the flow rate of the bioink in screw-driven bioprinting is affected and/or regulated by the screw speed and/or printing pressure applied to the bioink reservoir, as well as the screw geometry and flow behavior. In piston-driven systems, under the assumption that the bioink is incompressible, the flow rate of the bioink is only dependent on the piston movement and is independent of the properties of the bioink being printed [7]. As such, piston-driven bioprinting can provide the best control over the flow rate compared to pneumatic- and screw-driven bioprinting.

4.2. Profile and structure of printed constructs

During the bioprinting process, bioink is deposited or printed on the printing stage. However, the bioink, once printed on the stage, is still in a solution or semi-solution form. Due to the effect of gravity, the bioink can flow or spread, thus mixing or fusing at the intersection of strands or deforming where upper strands span the gap between lower strands or hang over at their ends. As a result, the strand profile and scaffold structure become different from that designed, as shown in Fig. 7, where the top view (a) illustrates the variations in strand cross-section with different locations and the cross-sectional view (b) illustrates the deflection of strand and pore size in the vertical direction as well as the reduced height of the whole construct.

During the bioprinting of scaffolds, bioink is extruded from the needle as it is controlled to move in the horizonal plane according to the scaffold design. The speed the needle moves in the horizonal plane is important with respect to the cross-sectional size or profile of the strand formed on the printing stage. If the swelling of a strand exiting the needle is ignored, the bioink, once extruded, forms a cylindrical filament with a diameter (D) governed by the flow rate (Q) of bioink extruded from the nozzle and nozzle moving speed (V) [246], i.e.,

$$D = \sqrt{4Q/(\pi V)} \quad (4)$$

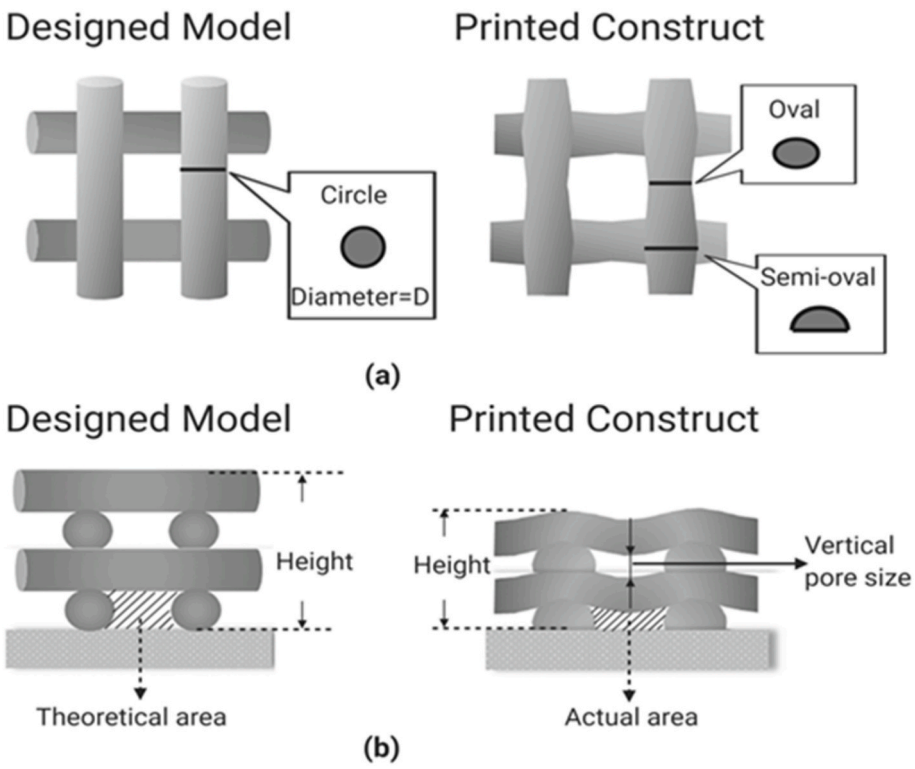

Fig. 7. Difference in strand profile between designed and printed scaffold structures: (a) top view and (b) cross-sectional view.

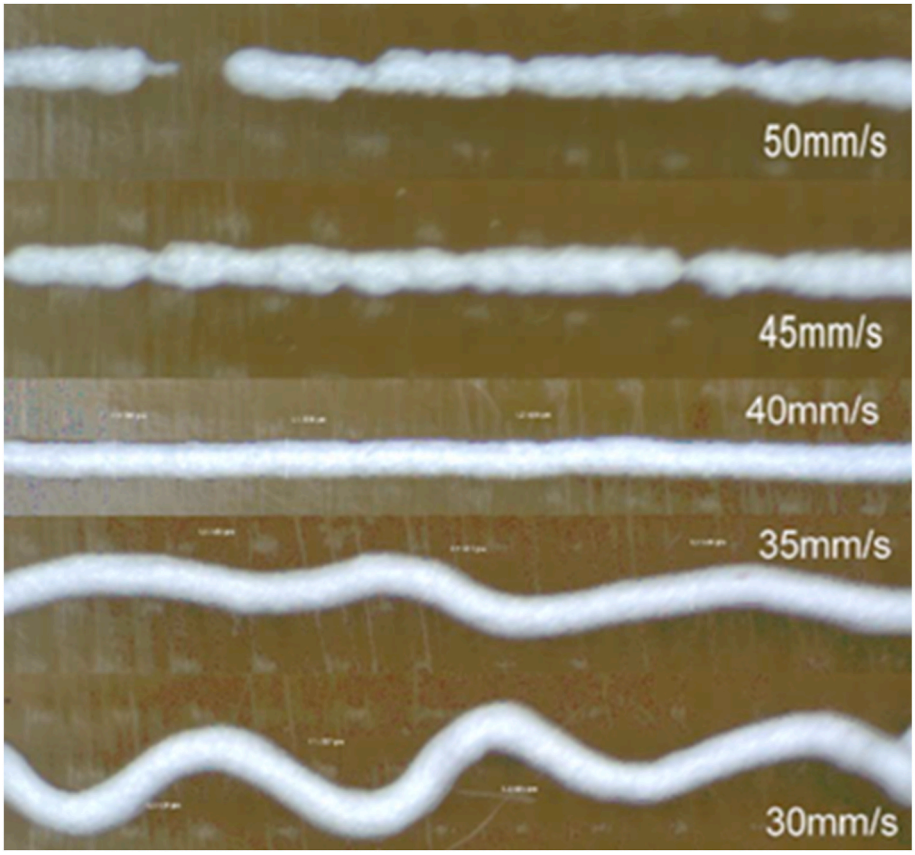

Fig. 8. Effect of needle speed on the printed stands, where the SF speed is around 40 mm/s [6,246].

The above equation shows that, for a given flow rate, the strand diameter is determined by the needle speed. Note that the use of a particular needle speed will ensure the diameter of the printed strand is equal to the internal diameter of the bioprinting needle if swelling of the material is neglected; such a speed is termed the stress-free (SF) speed as there is no stress induced within the strand. If the selected needle speed is faster than the SF speed, the printed strand will stretch to induce a tensile stress within the strand, resulting in a strand diameter smaller than the needle; the converse also holds. Fig. 8 shows the dependance of printed strands on the needle speed, where the SF speed is about 40 mm/s [246]. If the selected needle speed is too high, the continuity of the strand may not be maintained due to the tensile stress induced within the stand, causing the strand to break. On the other hand, lowering the needle speed below the SF speed induces compressive stress within the strand, leading to irregular stand orientation and increased strand diameter. If the needle speed becomes too low, printing a straight strand becomes difficult due to the induced compression.

4.3. Process-induced forces and cell damage

During the bioprinting process, cells are subjected to sustained process-induced forces, such as pressure, shear stress, and extensional stress, which cause the deformation and breach of cell membranes. Although cells have the elastic capability to resist a certain level of mechanical force, cell membranes may lose their integrity if the applied force exceeds a certain threshold; as a result, cells may be damaged and even lose their functionality and viability [103,106]. A compressive force on cells is generated due to hydrostatic pressure when cells are suspended in solution (Fig. 9a). During bioprinting, the compressed air creates forces on the cell suspension loaded in the syringe, with the corresponding hydrostatic pressure approximately equaling the bioprinting pressure (if the pressure drop in the syringe can be ignored). Hydrostatic pressure is also present in the needle, the magnitude of which is dependent on the location of cells inside the needle, as given by [287].

$$P_n(l) = \left(1 - \frac{l}{L_n}\right)\Delta P \tag{5}$$

where ΔP is the pressure drop along the needle, L_n is the needle length, and l is the distance from the needle entrance to the location of cells inside the needle ($0 < l < L_n$).

Shear stress is a mechanical force that introduces cell damage during bioprinting. Considering the diameter of the syringe is much greater than the needle tip diameter, the bioink flow inside the syringe can be neglected and therefore the bioprinting process-induced shear stress is predominantly distributed inside the narrow needle tip as the cell suspension is forced to flow through (Fig. 9b, where we consider the yield stress is zero for simplicity so no plug flow region of velocity is involved) and given by

$$\tau = \left(\frac{r}{2}\right)\left(\frac{\Delta P}{L}\right) \tag{6}$$

where r is the radial distance from the tip center to the location where the shear stress is measured ($0 \le r \le R$, where R is the needle radius). The above equation shows that shear stress in the needle tip is dependent on the pressure drop and the needle length, and shear stress is linearly distributed along the radial direction inside the needle considering a fully developed flow and no slip at the needle wall. For a given pressure and needle length, the shear stress reaches a maximum value at the needle wall and decreases to zero at the center of the needle.

Another mechanical force to which cells are subjected is extensional stress, which is a tensile stress generated due to the extensional flow field. Extensional flow is induced at the region of abrupt contraction of the needle, where the solution velocity difference before and after the contractive region is large (Fig. 9c). There are several ways to express the extensional stress in the contractive region, such as by measuring the extensional velocities [294] or detecting the pressure drop in the contractive region [295]. Detecting the pressure drop is an easier approach to perform which assumes the pressure drop in the coni-cylindrical entrance are resulted from shear flow and extensional flow and these terms are additive [295]. Based on this assumption, the fluid would adopt a contractive profile to minimize the total pressure drop, with the fluid having an extensional viscosity independent of the extensional rate while the shear viscosity is a power-law function of the shear rate. Thus, the expression for the extensional stress is

$$\tau_e = \frac{3}{8}(n+1)P_{en} \tag{7}$$

where τ_e is the extensional stress, P_{en} is the pressure drop at the contractive region, and n is the power-law index for shear flow. This expression is only applicable in situations in which the entrance angle of the entrance region is sufficiently large so as to not interfere with the flow pattern. This can be only guaranteed for large angles that approach an abrupt or flat entry with an entrance angle of 90°. Also, the resulting extensional stress is an average value that cannot capture features of the flow from different streamlines in the region.

It would be noted that, due to the complexity of bioprinting, it is difficult, or even impossible, to represent the process-induced forces and thus resulted in cell damage. Nowadays, machine learning comes into action for predicting cell viability [286,296] and optimizing printing parameters to improve the cell viability [297]. It is expected that machine learning, with the help of real-time monitoring and/or feedback, will allow for adjusting the printing parameters such as printing speed, pressure, and temperature as to preserve the cell viability or minimize cell damage.

4.4. Crosslinking in bioprinting

To create hydrogel-based 3D scaffolds with integrated structures, the hydrogel solution must be solidified or crosslinked to enhance the

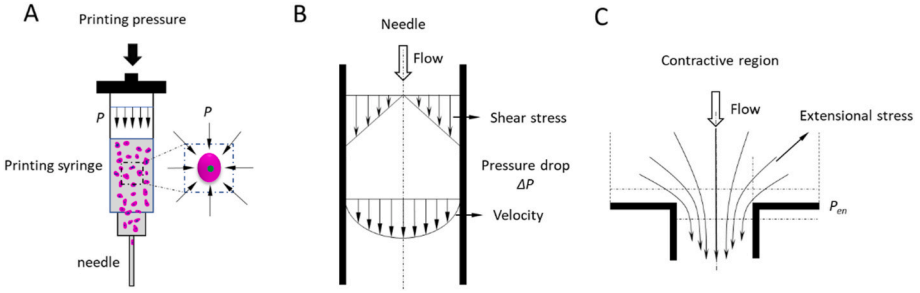

Fig. 9. Mechanical forces to which cells are subjected during bioprinting: (a) hydrostatic pressure; (b) shear stress (for simplicity, yield stress τ 0 = 0); and (c) extensional stress.

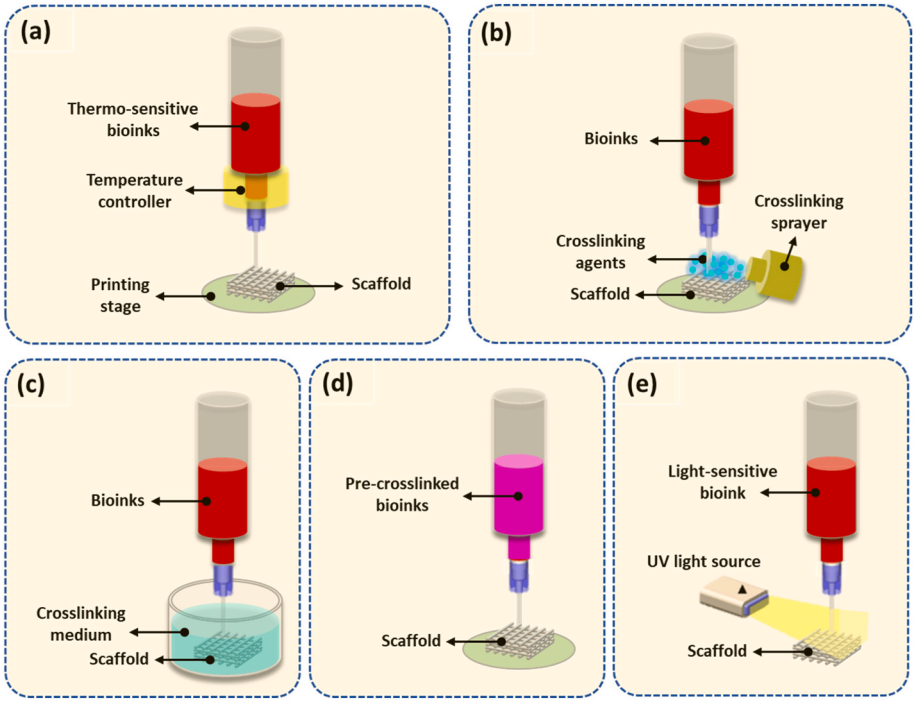

Fig. 10. Methods and configurations for hydrogel scaffold crosslinking. (a) crosslinking under temperature control; (b) crosslinking under spray; (c) crosslinking in medium bath; (d) pre-crosslinking; and (e) crosslinking under a UV light.

Table 3
Crosslinking techniques in bioprinting.

Crosslinking techniques	Processes	Merits	Demerits	Ref.
Thermal crosslinking	The polymerization of bioinks is control via heating and cooling	Simple; can be controlled sustainably during the whole bioprinting process.	Longer crosslinking time; the degree of crosslinking is hard to be precisely tuned; may adversely affects the function of cells.	[298–300]
Atomized crosslinking	The crosslinking agents are atomized and sprayed onto the bioprinted element/structure	Rapid crosslinking reaction in contact; simple setup.	The control to allow homogeneous distribution of the atomized agent is challenging; relatively slow gelation and incomplete crosslinking; not easy to maintain structural fidelity and stability for bioinks with weak mechanical properties	[301–304]
Bioplotting	Bioinks are deposited directly into the crosslinking bath	Provides sufficient crosslinking agents; trigger homogeneous gelation in a bath; rapid solidification; high printing fidelity.	Requires the careful adjustment of crosslinking agents to balance buoyancy of the crosslinking medium, as well as the gelation rate by tailoring the concentration of crosslinking agent to ensure the formation of printouts with high structural accuracy.	[305–307]
Pre-crosslinking	Introducing gelled particles via either thermal, ionic or covalent crosslinking in bioinks before deposition.	Increases the viscosity of a bioink and therefore the deposition quality; the structural stability of can then be easily achieved.	Increased printing pressure which may adversely affect cells; lead to an uneven distribution of formed hydrogel particles, thus discontinuities and nonuniformities in printed filaments.	[308–311]
UV crosslinking	The polymerization of bioinks is initiated by external UV light in bioprinting	Increases printing fidelity when using low viscosity bioinks.	Harmful for cells; transparency and fragile printing nozzle is needed.	[312–314]

mechanical strength and stability. Crosslinking can be initiated by means of physical stimuli or chemically induced via a crosslinking agent or enzymatic reaction. Among such methods, the most commonly used for bioprinting are ionic, thermal, and photo crosslinking, as discussed in Section 3.3. Depending on hydrogel properties, various crosslinking methods with associated configurations have been developed for bioprinting, as shown in Fig. 10, along with their merits and demerits listed in Table 3.

By manipulating the temperature of thermo-sensitive bioinks, such as those based on agarose, gelatin, or collagen, before and after printing, thermal crosslinking of the bioink can take place in the bioprinting process. Fig. 10a shows a configuration where the temperature of the bioink in the syringe is controlled above the melting temperature of the bioink to retain its solution form and the temperature of the printing stage is set to below the gelation temperature so that the bioink, once printed, gels on the stage. As such, the crosslinking process requires a temperature-regulation controller installed in the bioprinting system. Ionic crosslinking is reversible and has been extensively applied for hydrogels such as alginate and chitosan. Gelation occurs upon the formation of ionic bonds after the polymer molecules encounter the crosslinking agent. Chemical crosslinking is similar to ionic crosslinking, where hydrogel solutions and crosslinking agents must come into contact. The formation of hydrogels is triggered by the crosslinker, which connects hydrogel molecules via covalent chemical bonds. One approach developed to introduce crosslinking agents is to atomize and then spray them onto the extruded hydrogel solution (Fig. 10b). Challenges related to this method include the control of atomized agents to allow homogeneous distribution on extruded solutions to form strands

with uniform diameter, as well as relatively slow gelation and incomplete crosslinking due to the limited effectiveness of the atomized crosslinking agent. Thus, maintaining structural fidelity and stability becomes difficult, especially when hydrogel precursors with poor mechanical properties such as low viscosities are utilized. To address these issues, hydrogel solutions can be deposited into a bath containing crosslinking medium (Fig. 10c). As sufficient crosslinking agents are homogeneously provided in the bath, the surface of the deposited solution that contacts the crosslinkers is rapidly solidified, limiting the spread of the hydrogel solution and thus supporting the fidelity of printed strands. This method is also known as 3D bioplotting and requires the careful adjustment of crosslinking agents because the buoyancy of the crosslinking medium may lead to the failure of scaffold stacking if an inappropriate crosslinking solution is utilized. An excessive gelation rate introduced by a high concentration of crosslinking agent would result in rapid stiffening of the strand surface, which may reduce the connection between adjacent layers and lead to poor scaffold stability. On the other hand, slow gelation speeds caused by a low concentration of crosslinker will result in poor fidelity of the printed strands due to solution spreading as well as poor mechanical properties and even failure to support the printed structure [63]. Pre-crosslinking, by adding and mixing low concentrations of crosslinking agent into the hydrogel solution, can also be applied for hydrogel-based bioprinting (Fig. 10d). The pre-crosslinking method introduces hydrogel particles in the hydrogel solution, which increases its viscosity and therefore the deposition quality. The structural stability of printed scaffolds can then be easily achieved by exposing the printed scaffold to a high concentration of crosslinker solution. The mechanical properties of pre-crosslinked scaffolds are good, but the printing pressure required during bioprinting increases relative to the viscosity of the pre-crosslinked hydrogel. In addition, pre-crosslinking introduces an uneven distribution of hydrogel particles in the hydrogel solution, leading to discontinuities and nonuniformities during extrusion. A UV light beam can be used in bioprinting to initiate hydrogel photopolymerization (Fig. 10e). A hydrogel can be photopolymerized in the presence of photoinitiators under lights. When the light source is used, the interaction of the light source and light-sensitive compounds (photoinitiators) initiates polymerization. For example, gelatin is an inexpensive, denatured collagen that retains an abundance of integrin-binding motifs and matrix metalloproteinase-sensitive groups that promote adhesion of cells. By adding methacrylate and methacrylamide groups to the amine-containing side groups, gelatin becomes gelatin methacryloyl (GelMA), a photopolymerizable material. GelMA maintains the thermo-sensitive properties of gelatin and can be gelled under temperature control, but can also be permanently polymerized upon exposure to UV light. As such, extrusion-based bioprinting in combination with a UV light source can be used to produce a GelMA-based scaffold.

5. Key issues and future advances in extrusion bioprinting

5.1. Key issues in extrusion bioprinting

Printability is one of key issues in extrusion bioprinting. Notably, during the bioprinting process, bioinks, once printed, are still in solution or semi-solution form, which can flow or spread on the print bed; as a result, the printed structure may become different from its design (Fig. 7); the degree of such a difference is used to characterize one perspective of bioprinting performance, termed printability [285,286,315]. Standardized methods to quantify printability have yet to be defined; however, common methods combine examination of printability in terms of extrudability, filament fidelity, and structural integrity [285,316,317]. Extrudability refers to the ability to extrude the bioink through a needle to form a continuous filament in a controlled manner (Fig. 8) under appropriate printing conditions or parameters [316]. This is often determined through testing various combinations of printing parameters including needle diameter, print speed, and pressure, and then analyzing the dimensions and consistency of the printed strands [316]. Filament fidelity refers to the difference in the cross-section between filaments formed on the printing stage and the printing needle cross-section [6,246,287]. As shown in Fig. 7, the cross-sectional profile of the filament formed may vary significantly depending on the layer and location leading to strands having a maximum and minimum diameter, and differing heights. The difference between these two dimensions provides a quantitative measure of printability based on filament fidelity [94]. Structural integrity defines the capability to maintain the 3D structure post-printing with dimensions like that of the design [316]. Structural integrity is degraded as the printed filaments become fused at strand intersections or deformed by hanging-over the adjacent layers below, which results in a difference from the designed structure in terms of the thickness of each individual layer, height of the whole construct, and/or pore size in all directions.

Printability can be affected by many factors, including the properties of the formulated bioinks, and parameters of the selected printing parameters. Surface tension and wettability are two other important physical parameters that affect the printability as they influence the formation of first layer, as shown in Fig. 3. Notably, most printing stages, composed of glass or plastic, have large contact angles with the printed hydrogel and, as such, establishing an anchor between the printed structure and printing surface is difficult. This issue can be overcome by either printing hydrogels in a hydrophobic high-density media, such as perfluorotributylamine, to decrease the contact angle when printing, or coating the printing surface with a thin layer of chemicals [41,63,318], such as 3-(trimethoxysilyl) propyl methacrylate or polyethyleneimine, to modify the printing surface properties for a decreased contact angle. Notably, although deemed significant in the formation of the fluid profile, the effect of surface tension and contact angle of bioinks on printability have not been investigated and elucidated [247]. Research has shown that the rheological behavior of a bioink has a significant effect on its printability [285,315]. On one hand, the more viscous the bioink solution, the better the printability as a high viscosity tends to reduce bioink flow/spreading. On the other hand, encapsulated cells survive better in less viscous bioink solutions and less viscous bioinks require relatively small mechanical forces for bioprinting, thus reducing process-induced forces and preserving cell viability. In addition, the bioink viscosities vary with the shear rate, termed as the shear-thinning/thixotropic behaviors. Shear-thinning behavior is often desired in bioprinting since, during the printing process, bioinks with shear-thinning behavior become less viscous as the shear rate increases [319]. As the shear stress is removed after exiting the nozzle, the bioink viscosity rapidly recovers, leading to high filament fidelity. Research has also illustrated that the crosslinking mechanism used and the mechanical properties of the bioink once crosslinked have significant effects on both cell viability and printability [320]. Rapid crosslinking of the bioink is desired for optimal printability; therefore, immediate crosslinking of the bioink upon printing is a common to maintain printed structures. Insufficiently crosslinked or mechanically weak hydrogel structures will undergo structural change and may collapse. In the context of bioprinting, the loss angle of the bioink (or tanδ) is known to directly impact printability [43,321].

Cell viability is another key issue of extrusion bioprinting. During the bioprinting process, cells are subjected to sustained process-induced forces, such as pressure, shear stress, and extensional stress, which cause the deformation and breach of cell membranes. Although cells have the elastic capability to resist a certain level of mechanical force, cell membranes may lose their integrity if the applied force exceeds a certain threshold; as a result, cells may be damaged and even lose their functionality and viability [287,290]. As previously discussed, an optimal bioink for a specific application must support cell adherence, migration, and proliferation, direct and/or control cellular differentiation, demonstrate limited immunogenicity, and have mechanical properties

similar to those of the tissue being mimicked, all while degrading at a rate compatible with cellular in-growth and ECM deposition [322,323]. All these traits must also be balanced with the printability of the bioink to allow for formation of high-resolution constructs with repeatable designs that support nutrient and waste transport [323]. As such, bioink development, cell incorporation, vascularization, and printing resolution are all highly interconnected; a number of issues or challenges remains to be addressed in the field of extrusion bioprinting.

Bioinks aim to mimic native tissues as closely as possible in order to support tissue function; however, native tissues consist of a complex network of various components including bioactive proteins and molecules (collagen, GAGs, laminin etc.), and growth factors [322]. While use of composite polymers is commonplace in developing bioinks with comparable mechanical properties to those of native tissues, these bioinks still lack many of the bioactive molecules found in native tissues. While researchers have been developing more complex bioinks with multiple components, this is often limited by the expense of the individual components, as well as the need to maintain printability [324]. The addition of dECM, which contains this complex network of bioactive components, is a promising strategy to increase the biological complexity of developed inks; however, use of dECM has its own challenges [322,325]. In many forms dECM lack printability, and while removal of all cellular and genetic material is one of the main goals of decellularization, balancing this complete removal while limiting damage to the ECM matrix is difficult [325]. Klak et al. recently developed a pancreatic dECM/gelatin methacrylate bioink and tested its mechanical properties, thermal stability and cytotoxicity before 3D extrusion printing pancreatic islets [326]. The printed scaffolds were then implanted in mice and their functionality was analyzed. It was found that the dECM containing bioink demonstrated three times greater functionality in terms of insulin secretion than the non-dECM containing material. As the likelihood of using extrusion bioprinting in clinical applications increases, ethical and safety concerns have also been raised about some biomaterial and cell culture conditions [324]. For example, Matrigel, which has been used widely across the field of tissue engineering, is sourced from the basement membrane of murine tumors [327,328]. Do to this, there is wide bath-to-batch variation and safety concerns with clinical translation [328]. Similar safety and ethical concerns have also been raised about the use of fetal calf serum (FCS) in cell culture [329]. Although FCS often allows for maintenance and active growth of various cell types for longer periods of time, the sourcing of FCS from unborn calves at the slaughterhouse has raised ethical concerns, as well as safety concerns due to a lack of reproducibility due to batch-to-batch variation [329].

Once a suitable biomaterial has been developed, researchers then face the challenge of cell selection. As a large number of cells are often required for incorporation into a bioink, cell lines are often used as they are relatively cheap and easily accessible; however, cell lines often lack functionality [323,330]. In order to overcome this, many researchers have moved to using primary cells or stem cells [331]. In these cases, researchers are reliant on cell donations to source cells, and control over cellular differentiation becomes a challenge based on culture conditions, bioink components, and external stimuli [331–333]. Co-culture of various cell types including epithelial, mesenchymal, immune, and endothelial cells has also been used to increase biological complexity [12]. Joshi et al. demonstrated the ability to use alginate-silk-based biomaterials to control the differentiation of human mesenchymal stem cells into two different lineages, chondrogenic and osteogenic, within the same scaffold through use of different bioinks [332]. It was demonstrated that increased phosphorylation of alginate increased osteogenic differentiation, while the addition of silk to the ink enhanced chondrogenic differentiation. Once cells have been incorporated into a bioprinted construct, their on-going growth and proliferation must be supported. The vascularization of 3D extrusion bioprinted constructs to support the required waste and nutrient transport is another on-going challenge. In the human body, each cell must sit within 200 μm of the nearest capillary in order to allow for waste and nutrient exchange and transport [334]. Within 3D printed constructs, this transport is commonly supported by the design and fabrication of interconnected porous networks that allow for cell media to permeate into the construct; however, printing resolution is limited, and these porous networks are a poor biomimetic substitute for the vasculature of native systems [335,336]. To overcome this, one method is to utilize multi-material bioprinting to form constructs, along with thermosensitive hydrogel that is then removed from the construct to form a vascular network with the help of endothelial cells [337].

While the technological capacity for higher printing resolution has been increasing rapidly, there are still many challenges in reaching cell-level printing resolution using extrusion based technologies, which may be necessary to recapitulate certain biological features such as capillaries or the air-blood barrier in the lungs [338]. The printing resolution of extrusion printing is tied to multiple factors including control over extrusion pressure/volume, needle size, and the rheological properties of the bioink. As discussed above, the printability of a biomaterial is related to its rheological properties, with more viscous bioinks generally demonstrating a higher degree of printability due to lesser spreading on the print bed. However, the higher pressure required to extrude viscous inks imposes larger process-induced forces, reducing cell viability. Due to this, the technological capacity to print very small resolution features, may not match up with the resolution of bioprinting [338]. Generally, a resolution of ~100 μm is considered to be the finest resolution extrusion bioprinting is capable of while still being a cell-friendly process [339]. Optimization of printing parameters for balancing printing resolution and cell viability is being carried out through experimental methods, modelling and numerical simulations. Phenomenological models have also been used to describe the degree of cell damage as a function of the needle employed and dispensing pressure, where the models fit the degree of cell damage with experimentally identified model coefficients for given cell types and printing conditions [315,340]. However, evaluating cell damage and viability corresponding to needle diameters and air pressure fails to capture the direct mechanism of mechanical stresses on cells. For improvement, one promising method is to quantify cell viability in the bioprinting process based on the cell damage laws. This method involves three steps [2,288]: (1) developing empirical models for cell damage or cell damage laws, which relate the percent cell damage to the mechanical force of hydrostatic pressure or shear/-extensive stress that cells experience (similar to Newton's second law that relates an object's motion to the mechanical force applied), (2) evaluating the mechanical forces that cells experience in every cell path in which they flow in the bioprinting process, and (3) determining the percent cell damage in all cell paths based on the results from the above steps, and then integrating them to obtain the overall percent cell damage in the bioprinting process and thereby the cell viability. Importantly, the resulting models can be used not only to describe the relationship between cell damage and bioprinting parameters, but also to form a basis to develop strategies to preserve the cell viability in bioprinting. Other advancements in 3D printing technologies and procedures including freeform reversible embedding are also being investigated for their ability to increase printing resolution [341].

5.2. Future advances in extrusion bioprinting

Biomimicry of native tissues that normally contain multiple cell types, extracellular matrix components, and other bioactive molecules, that are organized in complex structures to perform specific functions, is the main goal of extrusion bioprinting. For tissue regeneration, printed constructs are expected to mimic the complex structures or composition of targeted tissues and facilitate the recovery of functions [1,9,10,15,16,303,342–349]. To meet this goal, many techniques are under development that utilize multiple biomaterials, enhance printability, aid in vascularization, and help direct and control cellular growth. These recent developments and successes indicate directions of further

advancement of extrusion bioprinting as outlined below.

Multiple-biomaterial printing refers to the development of novel methods/tools for extrusion of multiple bioinks. These multi-material techniques will help overcome some of the limitations of standard extrusion printing by allowing for the printing of constructs with increased complexity that recapitulate native systems to a higher degree [350]. Different methods of multiple-biomaterial printing are being developed including utilization of multiple print heads, co-axial printing, and chaotic bioprinting.

Pre-mixing or blending various cell types in different bioinks and then utilizing multiple printing heads, with each printing one bioink, is one method for incorporation of multiple biomaterials [350]. Through control over the deposition of the individually loaded print heads, multiple bioinks can be printed at different locations and organized to form complex scaffolds [337]. Hybrid scaffolds, comprised of 3D structural frames that impart mechanical strength and a hydrogel network that incorporates living cells, are a common application of multi-material bioprinting. Tubular scaffolds for spinal cord repair were developed in this way, utilizing a 3D printed macroporous PCL and pre-linked alginate, as shown in Fig. 11 [351]. In another study, PCL beads were loaded into a high-temperature printing head and melted at a temperature of 65–80 °C, while a dissolved alginate-chondrocyte suspension was loaded into a low-temperature printing head maintained at 10 °C [352]. Each material was printed in an alternating pattern, forming a PCL-alginate-based hybrid scaffold with good structural stability owing to the strong support provided by the PCL, and high biocompatibility as the hydrogel was able to support cell functions including cell viability, proliferation, and cartilage differentiation.

While multi-material bioprinting is often done on standard extrusion printers, where the printer exchanges print heads between layers, other researchers have developed dual-arm systems to allows for concurrent printing with multiple print heads, as well as single print heads that allow for the loading of multiple bioinks into different chambers [337,350,353].

To mimic the heterogeneous structures of native tissues/organs, novel methods/tools to bioprint fibers with structures in which the distribution of biomaterials/cells can be controlled longitudinally and/or circumferentially are being developed. For this, an emerging technique is coaxial printing, in which a series of coaxial tubular channels for printing bioinks are constructed or assembled by inserting small-diameter needle(s) into large-diameter needle(s) [354]. The fibers produced by coaxial printing are composed of a series of coaxial tubular layers, with each layer made from a bioink or sacrificial material. Co-axial printing has facilitated the fabrication of scaffolds with advanced structures, such as those with vessel-like channels [347,355]. Due to this, co-axial printing has become very popular for fabrication of tubular structures such as vasculature, intestinal villi, hair follicles, and vascularized bone [355–357]. Investigation into the difference between creating homogeneous structures versus core shell structures for regenerating vascularized bone demonstrated that the core-shell structure, with a core of vascular cells and a shell of osteoblasts led to a significant increase in osteogenic and angiogenic factors, demonstrating the importance of cellular positioning and interactions for increased functionality [354].

Chaotic bioprinting is another promising technique for increasing print complexities and subsequent biological similarities [358]. In this technique, multiple materials, often a bioink and a sacrificial material are blended using chaotic advection, before being co-extruded through the same nozzle, as shown in Fig. 12 [358,359].

This results in a strand that has a mix of two materials, with a highly aligned microstructure, and in the case of a sacrificial material, microchannels can then be formed within a printed strand [359]. This technique has been adapted by researchers in the field of skeletal muscles due to the similitude of the formed structure to the native architecture of muscle, as well as the ability to promote vascularization [358,359]. Other promising methods include rapid continuous multi-material extrusion bioprinting, embedded multi-material bioprinting, and pre-set multiple material bioprinting [352,360–362].

Embedded bioprinting is a class of advanced bioprinting techniques that utilize extrusion printing of bioinks directly into a medium containing bath, as shown in Fig. 13 [363]. Freeform reversible embedding (FRE) and FRE of a suspended hydrogel (FRESH) are emerging techniques that fall into this category [363,364]. Unlike bioplotting (as show in Fig. 10c, where the bath media causes cross-linking), the main function of the medium bath utilized in embedded bioprinting is for supporting the bioink once printed. While standard extrusion printing techniques often lack printability due to the need to balance viscosity with post-printing cell viability, embedded printing helps to overcome this challenge, allowing for extreme overhangs and more complex designs to be fabricated from less viscous bioinks [313,365,366]. In this way, embedded bioprinting can significantly enlarge the pool of bioinks that can be printed [367,368]. One challenge of embedded bioprinting is the one associated with the properties of the supportive medium. In addition to being non-toxic, biocompatible, non-permeable to the bioink and its components to minimize diffusion, the supporting medium must also possess the appropriate rheological properties, as characterized by yield stress and viscosity, to allow for the movement of the needle through the medium during printing while also being strong enough to support the printed construct without movement after printing [364,369]. In some cases, the support medium may also support the cross-linking of the construct [367]. Common supporting medias include Carbopol, hyaluronic acid, alginate/xanthan gum, gelatin/agarose/GelMA, and laponite [370]. For reversible forms of embedded bioprinting (FRE, FRESH) the supporting

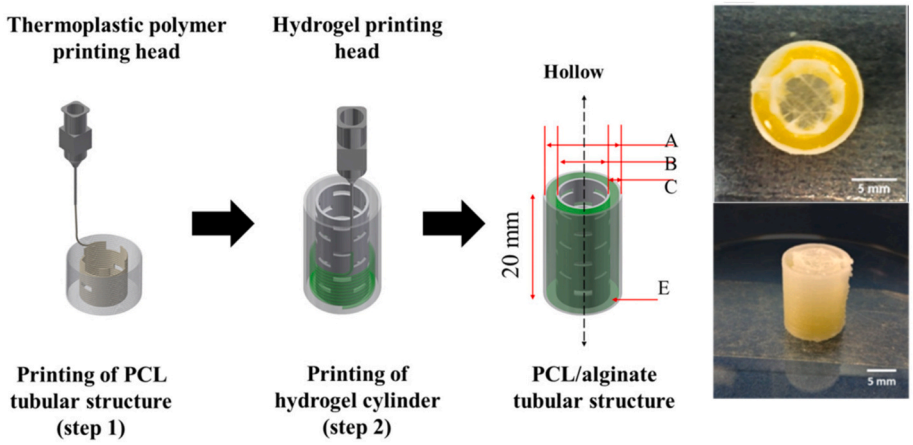

Fig. 11. An experimental example of multiple-biomaterial (i.e., PCL and alginate) printing with multiple printing heads [351].

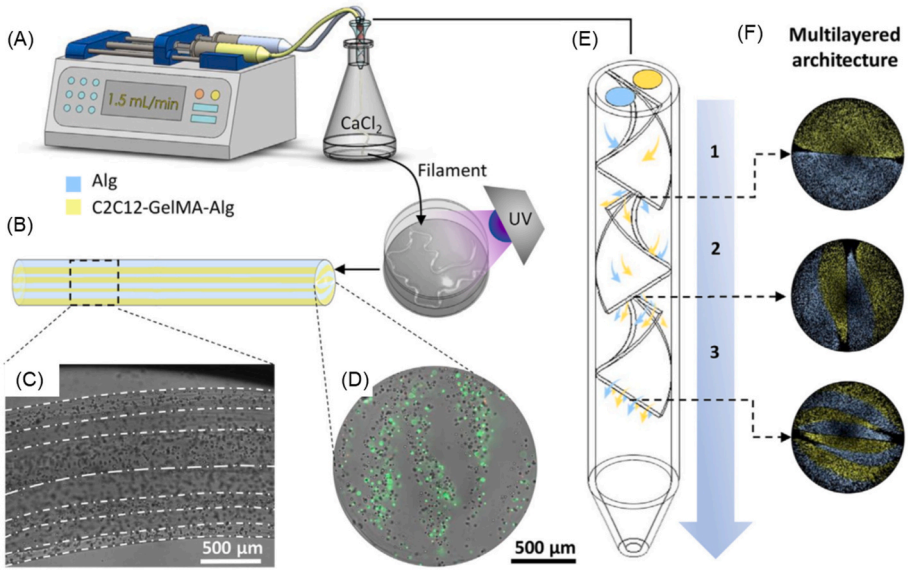

Fig. 12. Chaotic bioprinting. (A) Schematics of the chaotic bioprinting setup, (B) Extruded chaotical filament (alginate and C2C12-GalMA-Alg), (C) cross-sectional and (D) axial view of printed constructs with several viable C2C12 cells, (E) schematics of a printhead containing three Kenics static mixer (KSM) elements, and (F) the cross-section of the multilayered structure developed by each KSM element [358].

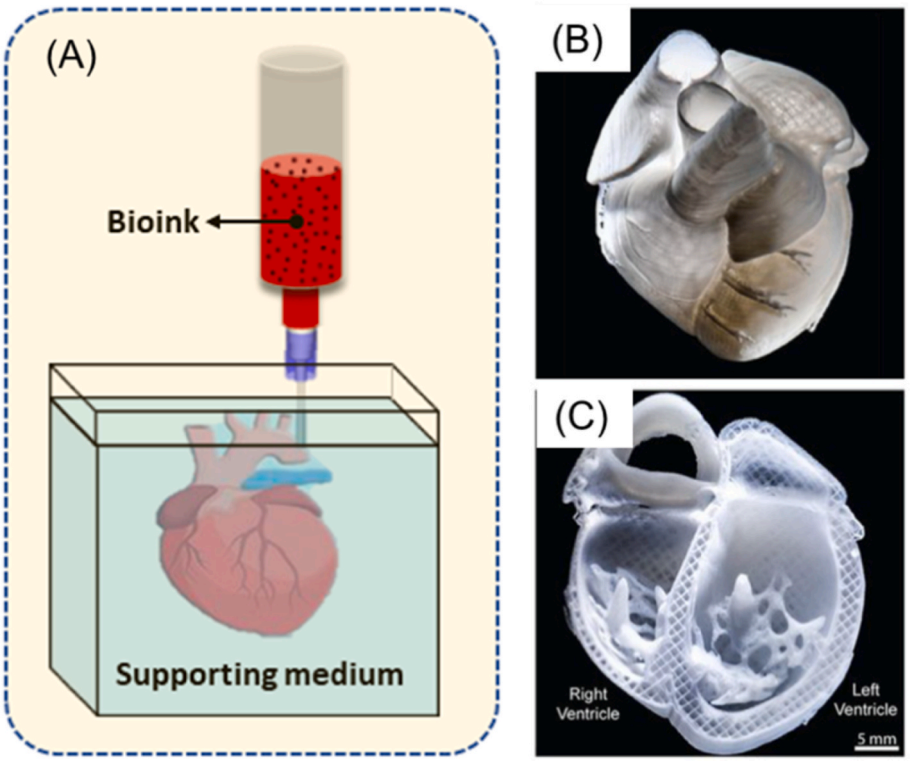

Fig. 13. Schematic of embedded bioprinting, (A) the bioink is printed into a supporting medium to form a complex 3D construct, (B) side view and (C) cross-sectional view of the printed heart model [371].

medium must also be easily removable to extract the printed construct [363]. Depending on the support medium properties, methods of removal include elevating the temperature to melt the medium, enzymatic cleavage, and simple washing or dilution. FRESH has been used in peripheral nerve regenerative engineering, as collagen is one of the primary bioinks of choice; however, collagen bioinks tend to exhibit very poor mechanical properties and structural fidelity [367]. Researchers successfully demonstrated the use of calcium ion incorporating gelatin as support medium for the printing of alginate/collagen bioinks incorporating human Schwann cells for peripheral nerve regeneration.

Hybrid bioprinting is a combinatorial method for scaffold fabrication that integrates extrusion-based bioprinting with other printing techniques. Such hybrid bioprinting capitalizes on the advantages of

extrusion-based bioprinting as well as other techniques to create scaffolds that could not be created by means of one bioprinting technique alone [264,372,373]. Integration of extrusion-based bioprinting with electrospinning provides enhanced capacity to produce complex scaffolds with varying scales of strands or fibers [372]. While the resolution of extrusion bioprinted strands is limited, electrospinning allows for the fabrication of fine fibers down to the nanometer scale (>200 nm) from polymer solutions or melts [374,375]. Using a system integrating these techniques, nano- or micro-scale fibers can be produced to create scaffolds with varying structures and environments. Such scaffolds may enhance the biological function, for example, by providing more cell-binding sites via nano-scale fibers that facilitate cell adhesion [374,375]. Scaffolds can also be fabricated with a zonal structure, where each zone is created by one technique with distinct structures and environments [376]. In development of nerve guided conduits, researchers used PLCL and PLGA scaffolds that consisted of a 3D extrusion printed outer wall, with an electrospun mesh on the inner wall, before being coated with polypyrrole, as shown in Fig. 14 [377]. Aortic arch vascular grafts have also been developed using hybrid techniques, with an original 3D framework being printed based on medical imaging, followed by an electrospinning of fibers over the graft framework [378]. The developed graft demonstrated functionality at physiological pressures and allowed infiltration of cells throughout the thickness of the graft.

Controlled release of biomolecules within printed constructs is of great importance for regulating the induction of biological activities, including cellular adhesion, proliferation, differentiation, and migration [379,380]. In tissue engineering, cells from patients or other sources are incorporated into printed scaffolds with the addition of bioactive molecules (or biomolecules), such as GFs, to trigger/promote cellular growth and/or functions. The scaffolds, once implanted into the damaged tissue/organ site, aid in cellular regeneration and recovery of tissue/organ function, with cell attachment, proliferation, and differentiation being key to successful tissue regeneration. GFs and other biomolecules activate sequential intracellular signaling pathways and control cellular gene expression [379,381]. As such, the dose, type, release rate, and timing of biomolecule availability affects the cellular response and function and thus must be appropriately regulated to promote regeneration of the desired tissue [379]. For this, various methods, or systems to incorporate or load the selected biomolecules into printed scaffolds have been developed. One promising method is to employ micro/nanoparticle delivery systems that protect the incorporated GFs and modulate their release profiles [382–389]. The particles employed can be structurally classified as micelles, dendrimers, liposomes, solid-lipid nanoparticles, and polymeric nanoparticles [383,386,390]. The size range of particles used in controlled release varies between 20 and 1000 nm and impacts the release kinetics of the loaded bioactive molecule. Among these systems, polymeric nanoparticles have several advantages including high stability, biodegradability, and flexibility in regulating the release rate of the GFs. Studies have begun to employ polymeric microparticles incorporating GFs to improve angiogenesis as well as the performance of target delivery systems [386–389]. The commonality in these studies is the use of micro-particles of single-layer polymers to encapsulate GFs, a technique that is severely undermined by the limited improvement in control over the release profile. By means of nano-technology, bi-layer nanoparticles were developed with the results demonstrating that sequential GF release (i.e., co-delivery of VEGF/bFGF followed by the release of PDGF) is feasible and controllable [388]. Achievements allowing for sequential GF release would represent a significant advance in the controlled release of GFs in tissue engineering. Further developing novel methods to achieve spatiotemporal release of GFs for promoting angiogenesis within printed constructs appears essential but to date remains unachievable [386,391].

Printing vascular networks within constructs is essential to maintain the viability and biological function of large cell populations within constructs. In vivo, well distributed vascular capillaries are seen in different tissues at every ~100–200 μm. Similarly, tissue regeneration with the aid of scaffolds or constructs, particularly large and thick scaffolds, requires the incorporation of an interconnected vascular network to facilitate mass transfer of nutrients, signaling molecules, oxygen, growth factors, metabolic waste, etc. between the cells in scaffolds and the culture medium [391–394]. To fabricate vascularized scaffolds, direct and indirect approaches based on bioprinting have been developed to create capillary-like structures or macro blood vessels [393,394]. Previously discussed techniques including co-axial nozzles, and chaotic bioprinting have garnered interest for their ability to directly form these vascular networks through the biofabrication of lumen-containing strands within scaffolds, analogous to native vessels [359,395]. In these approaches, cell/hydrogel mixtures are used as a bioink, while growth factors are often added to enhance the bio-functionality of the bioink [396,397]. In other indirect approaches, vascular networks are generated within the scaffold by removing sacrificial strands that are created by bioprinting or other additive manufacturing techniques [398]. To date, impressive progress in printing vascular scaffolds or constructs has been achieved; however, many issues still need to be addressed, in terms of biomaterial selection, cell viability and differentiation, and inclusion of growth factors, as well as methods to integrate these elements to form scaffolds or constructs with functional vascular networks.

Machine learning is a promising research direction for improving in extrusion bioprinting in many ways. Machine learning can be used to predict the properties of bioinks/scaffolds and optimize the printing

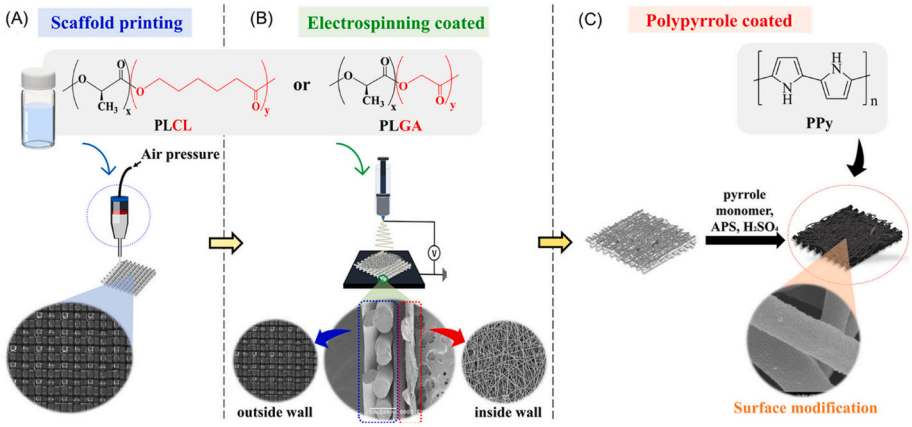

Fig. 14. Schematic diagram of a hybrid bioprinting technique for 3D/E/PPy scaffold fabrication: (A) scaffolds prepared by extrusion printing, (B) nanofiber covering on 3D printed scaffolds by electrospinning, and (c) deposition of PPy onto 3D/E scaffolds [377].

parameters, such as pressure, speed, and temperature, and to evaluate the printability and functionality of the bioinks [399–401]. M. One example of machine learning in extrusion bioprinting is the use of Bayesian optimization (BO) to optimize the bioprinting performance, such as the printability [402], based on prior knowledge and feedback. While it is true that many machine learning algorithms, especially for deep learning algorithms, require large amounts of data to be effective, recent advances in algorithms and computing capacity have made it possible to develop models based on smaller sample sizes. For example, task-specific models that are trained on a limited set of data can still yield accurate predictions or optimizations. Additionally, transfer learning techniques can be used to leverage knowledge from related domains to improve the performance of models even with limited data. Therefore, while data availability remains a challenge, the potential benefits of applying machine learning to extrusion bioprinting are significant and warrant further exploration.

6. Conclusions

Formulated from biomaterials and living cells, bioinks have been widely used in bioprinting to create 3D cell-incorporating constructs for biomedical engineering applications. Bioinks have been formulated or synthesized widely from polymers. Polymers are organic biomaterials possessing long chains with high water content, thus being able to provide a hydrated tissue-like environment that supports cell functions (including cell attachment, proliferation and differentiation) and tissue regeneration. Polymers are either natural or synthetic; natural polymers (e.g., alginate and collagen) have the intrinsic capability to support cell functions, while synthetic polymers (e.g., polycaprolactone (PCL) and polylactic acid (PLA)) are usually biologically inert but exhibit strong and robust mechanical properties [2]. While material science continues in developing and synthesizing new polymer bioinks with more appropriate properties for bioprinting, research has also begun to use two or more polymers or composite polymers to formulate bioinks. Also, composites with the incorporation of inorganic fillers for improved mechanical properties, electrical properties, and biological properties, have been drawing considerable attention for future advances.

For bioprinting, the flow rate of the printed biomaterial, strand profile and structure formed, process-induced forces, and crosslinking of the biomaterial solution, are all factors of importance that must be designed and regulated via the bioink flow properties, structural parameters (needle shape and size), and printing parameters (printing forces and needle movement). Notably, during the bioprinting process, cells are subjected to sustained process-induced forces, such as pressure, shear stress, and extensional stress, which cause the deformation and breach of cell membranes. Although cells have the elastic capability to resist a certain level of mechanical force, cell membranes may lose their integrity if the applied force exceeds a certain threshold; as a result, cells may be damaged and even lose their functionality and viability. Meanwhile, during the bioprinting process, bioinks, once printed, are still in solution or semi-solution form, which can flow or spread on the print bed. As a result, the printed structure may become different from its design. Printability is used to characterize the degree of such a difference.

Bioink properties and printing parameters are critical to bioprinting performance in terms of cell viability and printability. Research has shown that the rheological behavior of a bioink has a significant effect on its printability. The more viscous the bioink solution, the better printability it has as high viscosity tends to reduce the bioink flow/spreading. On the other hand, encapsulated cells survive better in less viscous bioink solutions and less viscous bioinks require relatively small mechanical forces for bioprinting, thus reducing process-induced forces, further preserving cell viability. Research has also illustrated that the bioink crosslinking mechanism used and the mechanical properties once crosslinked, have significant effects on both cell viability and printability. Rapid crosslinking of a bioink is desired to maintain printability. As the printed constructs provide cells with a biomechanical environment that supports cell functions and tissue regeneration, the degradation of the scaffold and subsequent decrease in mechanical strength must be balanced with the concurrent increase in mechanical strength caused by cell growth and tissue regeneration within the construct. It is generally accepted that the mechanical strength of a construct should be similar to that of the tissue/organ being repaired for best support of cell viability and other function, as well as tissue regeneration.

Bioprinting scaffolds with multiple materials and cells has attracted considerable attention related to efforts to mimic native tissue components. Various extrusion-based bioprinting techniques have been developed and advanced, such as embedded bioprinting, multi-head bioprinting, co-axial bioprinting, and hybrid bioprinting. More advanced extrusion-based bioprinting techniques are expected to be developed in the future for tissue-like scaffold fabrication.

Credit authorship contribution statement

X.B. Chen: Conceptualization, Methodology, Investigation, Supervision, Writing - Original Draft, Funding acquisition, Project administration. A. Fazel Anvari-Yazdi: Writing-review & editing, Writing - Revised Draft, Validation, Supervision. A. Zimmerling: Writing-review & editing, Validation. X. Duan: Writing-review & editing, Validation. R. Gharraei: Writing-review & editing, Validation, Data curation. N.K. Sharma: Writing-review & editing, Validation. S. Sweilem: Writing-review & editing, Validation. L. Ning: Writing – Original Draft, Writing – Revised Draft, Data curation, Investigation.

Ethics approval and consent to participate

There is no need for ethics approval and consent to participate, because this is a review paper without human or animal experiments.

Declaration of competing interest

The authors declare that they have no known competing financial interests or personal relationships that could have appeared to influence the work reported in this paper.

Acknowledgement

Support from the Natural Sciences and Engineering Research Council (NSERC) of Canada, the Canada Foundation for Innovation (CFI), and the Saskatchewan Health Research Foundation (SHRF) to the authors' work are acknowledged. The authors are also indebted to research collaborations and studies carried out within the Tissue Engineering Research Group (TERG) at the University of Saskatchewan.

Appendix A. Supplementary data

Supplementary data to this article can be found online at https://doi.org/10.1016/j.bioactmat.2023.06.006.

References

[1] S.V. Murphy, A. Atala, 3D bioprinting of tissues and organs, Nat. Biotechnol. 32 (8) (2014) 773–785.
[2] D.X. Chen, Extrusion bioprinting of scaffolds, in: Extrusion Bioprinting of Scaffolds for Tissue Engineering Applications, Springer, 2019, pp. 117–145.
[3] G. Decante, et al., Engineering bioinks for 3D bioprinting, Biofabrication 13 (3) (2021), 032001.
[4] Y.S. Zhang, et al., 3D extrusion bioprinting, Nature Reviews Methods Primers 1 (1) (2021) 75.
[5] L. Ning, et al., Process-induced cell damage: pneumatic versus screw-driven bioprinting, Biofabrication 12 (2) (2020), 025011.
[6] X. Chen, Modeling of Rotary Screw Fluid Dispensing Processes, 2007.
[7] X. Chen, J. Kai, Modeling of positive-displacement fluid dispensing processes, IEEE Trans. Electron. Packag. Manuf. 27 (3) (2004) 157–163.

[8] X. Chen, J. Kai, M. Hashemi, Evaluation of Fluid Dispensing Systems Using Axiomatic Design Principles, 2007.
[9] A. Zimmerling, Y. Zhou, X. Chen, Bioprinted constructs for respiratory tissue engineering, Bioprinting 24 (2021), e00177.
[10] A. Zimmerling, X. Chen, Bioprinting for combating infectious diseases, Bioprinting 20 (2020), e00104.
[11] J. Berg, et al., Optimization of cell-laden bioinks for 3D bioprinting and efficient infection with influenza A virus, Sci. Rep. 8 (1) (2018) 1–13.
[12] J. Berg, et al., Bioprinted multi-cell type lung model for the study of viral inhibitors, Viruses 13 (8) (2021) 1590.
[13] L.Y. Daikuara, et al., 3D bioprinting constructs to facilitate skin regeneration, Adv. Funct. Mater. 32 (3) (2022), 2105080.
[14] N.S. Lameirinhas, et al., Nanofibrillated cellulose/gellan gum hydrogel-based bioinks for 3D bioprinting of skin cells, Int. J. Biol. Macromol. 229 (2023) 849–860.
[15] H. Alizadeh Sardroud, X. Chen, B.F. Eames, Applied compressive strain governs hyaline-like cartilage versus fibrocartilage-like ECM produced within hydrogel constructs, Int. J. Mol. Sci. 24 (8) (2023) 7410.
[16] H. Alizadeh Sardroud, et al., Cartilage tissue engineering approaches need to assess fibrocartilage when hydrogel constructs are mechanically loaded, Front. Bioeng. Biotechnol. 9 (2022) 1388.
[17] A. Sadeghianmaryan, et al., Fabrication of chitosan/alginate/hydroxyapatite hybrid scaffolds using 3D printing and impregnating techniques for potential cartilage regeneration, Int. J. Biol. Macromol. 204 (2022) 62–75.
[18] Z. Yazdanpanah, et al., 3D bioprinted scaffolds for bone tissue engineering: state-of-the-art and emerging technologies, Front. Bioeng. Biotechnol. 10 (2022).
[19] T. Wang, et al., Tissue-specific hydrogels for three-dimensional printing and potential application in peripheral nerve regeneration, Tissue Eng. 28 (3–4) (2022) 161–174.
[20] K. Liu, et al., 3D printed personalized nerve guide conduits for precision repair of peripheral nerve defects, Adv. Sci. 9 (12) (2022), 2103875.
[21] F. Mohabatpour, et al., Bioprinting of alginate-carboxymethyl chitosan scaffolds for enamel tissue engineering in vitro, Biofabrication 15 (1) (2022), 015022.
[22] F. Mohabatpour, et al., Self-crosslinkable oxidized alginate-carboxymethyl chitosan hydrogels as an injectable cell carrier for in vitro dental enamel regeneration, J. Funct. Biomater. 13 (2) (2022) 71.
[23] S. Liu, et al., Three-dimensional Bioprinting Sodium Alginate/gelatin Scaffold Combined with Neural Stem Cells and Oligodendrocytes Markedly Promoting Nerve Regeneration after Spinal Cord Injury, vol. 9, Regenerative Biomaterials, 2022.
[24] J. Yang, et al., 3D bio-printed living nerve-like fibers refine the ecological niche for long-distance spinal cord injury regeneration, Bioact. Mater. 25 (2023) 160–175.
[25] R. Wang, et al., Remodelling 3D printed GelMA-HA corneal scaffolds by cornea stromal cells, Colloid and Interface Science Communications 49 (2022), 100632.
[26] M.R. Perez, et al., 3D-bioprinted cardiac tissues and their potential for disease modeling, Journal of 3D printing in medicine (2023) 3DP6.
[27] J. Bliley, et al., FRESH 3D bioprinting a contractile heart tube using human stem cell-derived cardiomyocytes, Biofabrication 14 (2) (2022), 024106.
[28] S.U. Ahmed, et al., Stentrievers: an engineering review, Intervent Neuroradiol. 29 (2) (2023) 125–133.
[29] C. Benwood, et al., Natural biomaterials and their use as bioinks for printing tissues, Bioengineering 8 (2) (2021) 27.
[30] E. Axpe, M.L. Oyen, Applications of alginate-based bioinks in 3D bioprinting, Int. J. Mol. Sci. 17 (12) (2016) 1976.
[31] M. Sarker, X. Chen, Modeling the flow behavior and flow rate of medium viscosity alginate for scaffold fabrication with a three-dimensional bioplotter, J. Manuf. Sci. Eng. 139 (8) (2017).
[32] S. Naghieh, et al., Influence of crosslinking on the mechanical behavior of 3D printed alginate scaffolds: experimental and numerical approaches, J. Mech. Behav. Biomed. Mater. 80 (2018) 111–118.
[33] J. Lee, et al., Bone-derived dECM/alginate bioink for fabricating a 3D cell-laden mesh structure for bone tissue engineering, Carbohydr. Polym. 250 (2020), 116914.
[34] L. Ning, et al., Influence of flow behavior of alginate–cell suspensions on cell viability and proliferation, Tissue Eng. C Methods 22 (7) (2016) 652–662.
[35] L. Ning, et al., Influence of mechanical properties of alginate-based substrates on the performance of Schwann cells in culture, J. Biomater. Sci. Polym. Ed. 27 (9) (2016) 898–915.
[36] M.A. Mendoza García, M. Izadifar, X. Chen, Evaluation of PBS treatment and PEI coating effects on surface morphology and cellular response of 3D-printed alginate scaffolds, J. Funct. Biomater. 8 (4) (2017) 48.
[37] M. Izadifar, et al., Bioprinting pattern-dependent electrical/mechanical behavior of cardiac alginate implants: characterization and ex vivo phase-contrast microtomography assessment, Tissue Eng. C Methods 23 (9) (2017) 548–564.
[38] M. Yeo, G. Kim, Electrohydrodynamic-direct-printed cell-laden microfibrous structure using alginate-based bioink for effective myotube formation, Carbohydrate Polym. 272 (2021), 118444.
[39] A. Rajaram, D.J. Schreyer, D.X. Chen, Use of the polycation polyethyleneimine to improve the physical properties of alginate–hyaluronic acid hydrogel during fabrication of tissue repair scaffolds, J. Biomater. Sci. Polym. Ed. 26 (7) (2015) 433–445.
[40] F. You, et al., Homogeneous hydroxyapatite/alginate composite hydrogel promotes calcified cartilage matrix deposition with potential for three-dimensional bioprinting, Biofabrication 11 (1) (2018), 015015.
[41] F. You, X. Wu, X. Chen, 3D printing of porous alginate/gelatin hydrogel scaffolds and their mechanical property characterization, International Journal of Polymeric Materials and Polymeric Biomaterials 66 (6) (2017) 299–306.
[42] F. You, et al., Bioprinting and in vitro characterization of alginate dialdehyde–gelatin hydrogel bio-ink, Bio-Design and Manufacturing 3 (1) (2020) 48–59.
[43] N. Soltan, et al., Printability and cell viability in bioprinting alginate dialdehyde-gelatin scaffolds, ACS Biomater. Sci. Eng. 5 (6) (2019) 2976–2987.
[44] M. Sarker, et al., Bio-fabrication of peptide-modified alginate scaffolds: printability, mechanical stability and neurite outgrowth assessments, Bioprinting 14 (2019), e00045.
[45] C.R. Jagadish, et al., Solubility of chitin: solvents, solution behaviors and their related mechanisms, in: X. Zhenbo (Ed.), Solubility of Polysaccharides, IntechOpen: Rijeka, 2017. Ch. 7.
[46] F. Mohabatpour, et al., Bioprinting of Alginate- Carboxymethyl Chitosan Scaffolds for Enamel Tissue Engineering in Vitro, Biofabrication, 2022.
[47] H.R. Bakhsheshi-Rad, et al., In vitro and in vivo evaluation of chitosan-alginate/gentamicin wound dressing nanofibrous with high antibacterial performance, Polym. Test. 82 (2020), 106298.
[48] H.R. Bakhsheshi-Rad, et al., Improved antibacterial properties of an Mg-Zn-Ca alloy coated with chitosan nanofibers incorporating silver sulfadiazine multiwall carbon nanotubes for bone implants, Polym. Adv. Technol. 30 (5) (2019) 1333–1339.
[49] A. Sadeghianmaryan, et al., Extrusion-based printing of chitosan scaffolds and their in vitro characterization for cartilage tissue engineering, Int. J. Biol. Macromol. 164 (2020) 3179–3192.
[50] S. Coşkun, et al., Formulation of chitosan and chitosan-nanoHAp bioinks and investigation of printability with optimized bioprinting parameters, Int. J. Biol. Macromol. 222 (2022) 1453–1464.
[51] M. Kołodziejska, et al., Chitosan as an underrated polymer in modern tissue engineering, Nanomaterials 11 (11) (2021) 3019.
[52] H.M. Butler, et al., Optimization of starch-and chitosan-based bio-inks for 3D bioprinting of scaffolds for neural cell growth, Materialia 12 (2020), 100737.
[53] M. Lazaridou, D.N. Bikiaris, D.A. Lamprou, 3D bioprinted chitosan-based hydrogel scaffolds in tissue engineering and localised drug delivery, Pharmaceutics 14 (9) (2022) 1978.
[54] Q. Liu, et al., Preparation and properties of 3D printed alginate–chitosan polyion complex hydrogels for tissue engineering, Polymers 10 (6) (2018) 664.
[55] G. Michailidou, et al., Preliminary evaluation of 3D printed chitosan/pectin constructs for biomedical applications, Mar. Drugs 19 (1) (2021) 36.
[56] H. Suo, et al., Low-temperature 3D printing of collagen and chitosan composite for tissue engineering, Mater. Sci. Eng. C 123 (2021), 111963.
[57] S. Maiz-Fernández, et al., 3D printable self-healing hyaluronic acid/chitosan polycomplex hydrogels with drug release capability, Int. J. Biol. Macromol. 188 (2021) 820–832.
[58] A. Dravid, et al., Development of agarose–gelatin bioinks for extrusion-based bioprinting and cell encapsulation, Biomed. Mater. 17 (5) (2022), 055001.
[59] S. Tarassoli, et al., Candidate bioinks for 3D bioprinting soft tissue, in: 3D Bioprinting for Reconstructive Surgery, Elsevier, 2018, pp. 145–172.
[60] T.K. Merceron, S.V. Murphy, Hydrogels for 3D bioprinting applications, in: Essentials of 3D Biofabrication and Translation, Elsevier, 2015, pp. 249–270.
[61] A.R. Yasin, et al., Filter extracted sliding mode approach for DC Microgrids, Electronics 10 (16) (2021) 1882.
[62] H.J. Faust, Q. Guo, J.H. Elisseeff, Cartilage tissue engineering, in: Principles of Regenerative Medicine, Elsevier, 2019, pp. 937–952.
[63] A. Rajaram, D. Schreyer, D. Chen, Bioplotting alginate/hyaluronic acid hydrogel scaffolds with structural integrity and preserved schwann cell viability, 3D Print. Addit. Manuf. 1 (4) (2014) 194–203.
[64] C.J. Little, W.M. Kulyk, X. Chen, The effect of chondroitin sulphate and hyaluronic acid on chondrocytes cultured within a fibrin-alginate hydrogel, J. Funct. Biomater. 5 (3) (2014) 197–210.
[65] M.-D. Wang, et al., Novel crosslinked alginate/hyaluronic acid hydrogels for nerve tissue engineering, Front. Mater. Sci. 7 (3) (2013) 269–284.
[66] C. Li, et al., Preparation and characterization of photocurable composite extracellular matrix-methacrylated hyaluronic acid bioink, J. Mater. Chem. B 10 (22) (2022) 4242–4253.
[67] J. Zhou, et al., Adaptive multifunctional supramolecular assemblies of glycopeptides rapidly enable morphogenesis, Biochemistry 57 (32) (2018) 4867–4879.
[68] X. Bai, et al., Fabrication of engineered heart tissue grafts from alginate/collagen barium composite microbeads, Biomed. Mater. 6 (4) (2011), 045002.
[69] M. Meyer, Processing of collagen based biomaterials and the resulting materials properties, Biomed. Eng. Online 18 (1) (2019) 1–74.
[70] Z. Li, C. Ruan, X. Niu, Collagen-based bioinks for regenerative medicine: fabrication, application and prospective, in: Medicine in Novel Technology and Devices, 2023, 100211.
[71] I.N. Amirrah, et al., A comprehensive review on collagen type I development of biomaterials for tissue engineering: from biosynthesis to bioscaffold, Biomedicines 10 (9) (2022) 2307.
[72] Y. Song, et al., Corneal bioprinting using a high concentration pure collagen I transparent bioink, Bioprinting 28 (2022), e00235.
[73] F. Netti, et al., Stabilizing gelatin-based bioinks under physiological conditions by incorporation of ethylene-glycol-conjugated Fmoc-FF peptides, Nanoscale 14 (23) (2022) 8525–8533.

[74] E. Yuce-Erarslan, et al., Photo-crosslinkable chitosan and gelatin-based nanohybrid bioinks for extrusion-based 3D-bioprinting, International Journal of Polymeric Materials and Polymeric Biomaterials 72 (1) (2023) 1–12.
[75] S. Yi, et al., Micropore-forming gelatin methacryloyl (GelMA) bioink toolbox 2.0: designable tunability and adaptability for 3D bioprinting applications, Small 18 (25) (2022), 2106357.
[76] T. Al Kayal, et al., Plasminogen-loaded fibrin scaffold as drug delivery system for wound healing applications, Pharmaceutics 14 (2) (2022) 251.
[77] K. Laki, The polymerization of proteins: the action of thrombin on fibrinogen, Arch. Biochem. Biophys. 726 (2022), 109244.
[78] S. England, et al., Bioprinted fibrin-factor XIII-hyaluronate hydrogel scaffolds with encapsulated Schwann cells and their in vitro characterization for use in nerve regeneration, Bioprinting 5 (2017) 1–9.
[79] J.K. Carrow, et al., Polymers for bioprinting, in: Essentials of 3D Biofabrication and Translation, Elsevier, 2015, pp. 229–248.
[80] M.Z. Albanna, J.H. Holmes IV, Skin Tissue Engineering and Regenerative Medicine, Academic Press, 2016.
[81] K. Yi, et al., Utilizing 3D Bioprinted Platelet-Rich Fibrin-Based Materials to Promote the Regeneration of Oral Soft Tissue, vol. 9, Regenerative Biomaterials, 2022.
[82] P. Pitacco, et al., 3D bioprinting of cartilaginous templates for large bone defect healing, Acta Biomater. 156 (2023) 61–74.
[83] X. Zhang, et al., Decellularized extracellular matrix scaffolds: recent trends and emerging strategies in tissue engineering, Bioact. Mater. 10 (2022) 15–31.
[84] A.D. McInnes, M.A. Moser, X. Chen, Preparation and use of decellularized extracellular matrix for tissue engineering, J. Funct. Biomater. 13 (4) (2022) 240.
[85] M. Sani, et al., Engineered artificial articular cartilage made of decellularized extracellular matrix by mechanical and IGF-1 stimulation, Biomaterials Advances 139 (2022), 213019.
[86] M. Latifi, et al., Fabrication of platelet-rich plasma heparin sulfate/hydroxyapatite/zirconia scaffold, Bioinspired, Biomimetic Nanobiomaterials 7 (2) (2018) 122–130.
[87] R. Asgarpour, E. Masaeli, S. Kermani, Development of meniscus-inspired 3D-printed PCL scaffolds engineered with chitosan/extracellular matrix hydrogel, Polym. Adv. Technol. 32 (12) (2021) 4721–4732.
[88] R. Binaymotlagh, et al., Peptide-based hydrogels: new materials for biosensing and biomedical applications, Materials 15 (17) (2022) 5871.
[89] X. Ding, et al., Synthetic peptide hydrogels as 3D scaffolds for tissue engineering, Adv. Drug Deliv. Rev. 160 (2020) 78–104.
[90] H. Jian, et al., Dipeptide self-assembled hydrogels with tunable mechanical properties and degradability for 3D bioprinting, ACS Appl. Mater. Interfaces 11 (50) (2019) 46419–46426.
[91] M. Dai, et al., Elastin-like polypeptide-based bioink: a promising alternative for 3D bioprinting, Biomacromolecules 22 (12) (2021) 4956–4966.
[92] T.L. Lopez-Silva, et al., Chemical functionality of multidomain peptide hydrogels governs early host immune response, Biomaterials 231 (2020), 119667.
[93] R. Khoeini, et al., Natural and synthetic bioinks for 3D bioprinting, Advanced NanoBiomed Research 1 (8) (2021), 2000097.
[94] A. Zimmerling, et al., 3D printing PCL/nHA bone scaffolds: exploring the influence of material synthesis techniques, Biomater. Res. 25 (1) (2021) 1–12.
[95] H.R. Bakhsheshi-Rad, et al., Antibacterial activity and corrosion resistance of Ta2O5 thin film and electrospun PCL/MgO-Ag nanofiber coatings on biodegradable Mg alloy implants, Ceram. Int. 45 (9) (2019) 11883–11892.
[96] N. Fazeli, et al., 3D-Printed PCL scaffolds coated with nanobioceramics enhance osteogenic differentiation of stem cells, ACS Omega 6 (51) (2021) 35284–35296.
[97] M.R. Dethe, et al., PCL-PEG copolymer based injectable thermosensitive hydrogels, J. Contr. Release 343 (2022) 217–236.
[98] S. Ramasamy, et al., Optimized construction of a full thickness human skin equivalent using 3D bioprinting and a PCL/collagen dermal scaffold, Bioprinting 21 (2021), e00123.
[99] M.A. El-Bakary, K.A. El-Farahaty, N.M. El-Sayed, Investigating the mechanical behavior of PGA/PCL copolymer surgical suture material using multiple-beam interference microscopy, Fibers Polym. 20 (2019) 1116–1124.
[100] A. Behl, et al., Biodegradable diblock copolymeric PEG-PCL nanoparticles: synthesis, characterization and applications as anticancer drug delivery agents, Polymer 207 (2020), 122901.
[101] A.D. Olubamiji, et al., Modulating mechanical behaviour of 3D-printed cartilage-mimetic PCL scaffolds: influence of molecular weight and pore geometry, Biofabrication 8 (2) (2016), 025020.
[102] A. Azari, et al., Deposition of crystalline hydroxyapatite nano-particle on zirconia ceramic: a potential solution for the poor bonding characteristic of zirconia ceramics to resin cement, J. Mater. Sci. Mater. Med. 28 (7) (2017) 1–8.
[103] A. Azari, et al., Deposition of crystalline hydroxyapatite nanoparticles on Y-TZP ceramic: a potential solution to enhance bonding characteristics of Y-TZP ceramics, J. Dent. 14 (2) (2017) 62.
[104] N. Salehi-Nik, et al., Polymers for oral and dental tissue engineering, in: Biomaterials for Oral and Dental Tissue Engineering, Elsevier, 2017, pp. 25–46.
[105] M. Feldman, L.S. Friedman, L.J. Brandt, Sleisenger and Fordtran's Gastrointestinal and Liver Disease: Pathophysiology, Diagnosis, Management, Elsevier health sciences, 2020.
[106] M. Monfared, et al., 3D bioprinting of dual-crosslinked nanocellulose hydrogels for tissue engineering applications, J. Mater. Chem. B 9 (31) (2021) 6163–6175.
[107] A. Bandyopadhyay, B.B. Mandal, N. Bhardwaj, 3D bioprinting of photo-crosslinkable silk methacrylate (SilMA)-polyethylene glycol diacrylate (PEGDA) bioink for cartilage tissue engineering, J. Biomed. Mater. Res. 110 (4) (2022) 884–898.
[108] L. Ouyang, et al., MMP-sensitive PEG hydrogel modified with RGD promotes bFGF, VEGF and EPC-mediated angiogenesis, Exp. Ther. Med. 18 (4) (2019) 2933–2941.
[109] H. Deng, et al., Injectable thermosensitive hydrogel systems based on functional PEG/PCL block polymer for local drug delivery, J. Contr. Release 297 (2019) 60–70.
[110] P.J. Kondiah, et al., A 3D bioprinted pseudo-bone drug delivery scaffold for bone tissue engineering, Pharmaceutics 12 (2) (2020) 166.
[111] Y. Wu, et al., 3D bioprinting of novel biocompatible scaffolds for endothelial cell repair, Polymers 11 (12) (2019) 1924.
[112] H. Bearat, B. Vernon, Environmentally responsive injectable materials, in: Injectable Biomaterials, Elsevier, 2011, pp. 263–297.
[113] E.V. Batrakova, A.V. Kabanov, Pluronic block copolymers: evolution of drug delivery concept from inert nanocarriers to biological response modifiers, J. Contr. Release 130 (2) (2008) 98–106.
[114] W. Boonlai, et al., Development and characterization of pluronic F127 and methylcellulose based hydrogels for 3D bioprinting, Polym. Bull. 80 (4) (2023) 4555–4572.
[115] P. Sungkhaphan, et al., Pluronic-F127 and Click chemistry-based injectable biodegradable hydrogels with controlled mechanical properties for cell encapsulation, React. Funct. Polym. 181 (2022), 105439.
[116] R. Suntornnond, et al., A highly printable and biocompatible hydrogel composite for direct printing of soft and perfusable vasculature-like structures, Sci. Rep. 7 (1) (2017) 1–11.
[117] M.N. Collins, et al., Scaffold fabrication technologies and structure/function properties in bone tissue engineering, Adv. Funct. Mater. 31 (21) (2021), 2010609.
[118] M. Maisani, et al., A new composite hydrogel combining the biological properties of collagen with the mechanical properties of a supramolecular scaffold for bone tissue engineering, Journal of tissue engineering and regenerative medicine 12 (3) (2018) e1489–e1500.
[119] M. Baniasadi, M. Minary-Jolandan, Alginate-collagen fibril composite hydrogel, Materials 8 (2) (2015) 799–814.
[120] F. Ketabat, et al., Optimization of 3D printing and in vitro characterization of alginate/gelatin lattice and angular scaffolds for potential cardiac tissue engineering, Front. Bioeng. Biotechnol. 11 (2023) 776.
[121] M.H. Kim, et al., Injectable methylcellulose hydrogel containing calcium phosphate nanoparticles for bone regeneration, Int. J. Biol. Macromol. 109 (2018) 57–64.
[122] S.R. Shin, et al., Reduced graphene oxide-gelMA hybrid hydrogels as scaffolds for cardiac tissue engineering, Small 12 (27) (2016) 3677–3689.
[123] C.-T. Huang, et al., A graphene–polyurethane composite hydrogel as a potential bioink for 3D bioprinting and differentiation of neural stem cells, J. Mater. Chem. B 5 (44) (2017) 8854–8864.
[124] M. Izadifar, et al., UV-assisted 3D bioprinting of nanoreinforced hybrid cardiac patch for myocardial tissue engineering, Tissue Eng. C Methods 24 (2) (2018) 74–88.
[125] A. Serafin, et al., Printable alginate/gelatin hydrogel reinforced with carbon nanofibers as electrically conductive scaffolds for tissue engineering, Mater. Sci. Eng. C 122 (2021), 111927.
[126] M. Ghanbari, et al., The impact of zirconium oxide nanoparticles content on alginate dialdehyde-gelatin scaffolds in cartilage tissue engineering, J. Mol. Liq. 335 (2021), 116531.
[127] M. Monavari, et al., 3D printing of alginate dialdehyde-gelatin (ADA-GEL) hydrogels incorporating phytotherapeutic icariin loaded mesoporous SiO2-CaO nanoparticles for bone tissue engineering, Mater. Sci. Eng. C 131 (2021), 112470.
[128] Z. Emami, et al., Modified hydroxyapatite nanoparticles reinforced nanocomposite hydrogels based on gelatin/oxidized alginate via Schiff base reaction, Carbohydrate Polymer Technologies and Applications 2 (2021), 100056.
[129] Z. Li, et al., Tuning alginate-gelatin bioink properties by varying solvent and their impact on stem cell behavior, Sci. Rep. 8 (1) (2018) 1–8.
[130] M. Sarker, et al., Influence of ionic crosslinkers (Ca2+/Ba2+/Zn2+) on the mechanical and biological properties of 3D Bioplotted Hydrogel Scaffolds, J. Biomater. Sci. Polym. Ed. 29 (10) (2018) 1126–1154.
[131] C. Hu, et al., Ions-induced gelation of alginate: mechanisms and applications, Int. J. Biol. Macromol. 177 (2021) 578–588.
[132] J.-Y. Wang, et al., Novel calcium-alginate capsules with aqueous core and thermo-responsive membrane, J. Colloid Interface Sci. 353 (1) (2011) 61–68.
[133] M. Neufurth, et al., Engineering a morphogenetically active hydrogel for bioprinting of bioartificial tissue derived from human osteoblast-like SaOS-2 cells, Biomaterials 35 (31) (2014) 8810–8819.
[134] D. Chimene, et al., Advanced bioinks for 3D printing: a materials science perspective, Ann. Biomed. Eng. 44 (6) (2016) 2090–2102.
[135] L.K. Narayanan, et al., 3D-Bioprinting of polylactic acid (PLA) nanofiber–alginate hydrogel bioink containing human adipose-derived stem cells, ACS Biomater. Sci. Eng. 2 (10) (2016) 1732–1742.
[136] F. You, et al., 3D printing of porous cell-laden hydrogel constructs for potential applications in cartilage tissue engineering, ACS Biomater. Sci. Eng. 2 (7) (2016) 1200–1210.
[137] Y. Luo, et al., 3D bioprinting scaffold using alginate/polyvinyl alcohol bioinks, Mater. Lett. 189 (2017) 295–298.
[138] J. Park, et al., Cell-laden 3D bioprinting hydrogel matrix depending on different compositions for soft tissue engineering: characterization and evaluation, Mater. Sci. Eng. C 71 (2017) 678–684.

[139] A. Aldaadaa, N. Owji, J. Knowles, Three-dimensional printing in maxillofacial surgery: hype versus reality, J. Tissue Eng. 9 (2018), 2041731418770909.
[140] M.D. Giuseppe, et al., Mechanical behaviour of alginate-gelatin hydrogels for 3D bioprinting, J. Mech. Behav. Biomed. Mater. 79 (2018) 150–157.
[141] M. Milazzo, et al., Additive manufacturing approaches for hydroxyapatite-reinforced composites, Adv. Funct. Mater. 29 (35) (2019), 1903055.
[142] D.R. Sahoo, T. Biswal, Alginate and its application to tissue engineering, SN Appl. Sci. 3 (1) (2021) 30.
[143] K.V. Harish Prashanth, R.N. Tharanathan, Crosslinked chitosan—preparation and characterization, Carbohydr. Res. 341 (1) (2006) 169–173.
[144] J.K. Francis Suh, H.W.T. Matthew, Application of chitosan-based polysaccharide biomaterials in cartilage tissue engineering: a review, Biomaterials 21 (24) (2000) 2589–2598.
[145] R.A.A. Muzzarelli, et al., Chitosan, hyaluronan and chondroitin sulfate in tissue engineering for cartilage regeneration: a review, Carbohydrate Polym. 89 (3) (2012) 723–739.
[146] T.T. Demirtaş, G. Irmak, M. Gümüşderelioğlu, A bioprintable form of chitosan hydrogel for bone tissue engineering, Biofabrication 9 (3) (2017), 035003.
[147] P.S. Bakshi, et al., Chitosan as an environment friendly biomaterial – a review on recent modifications and applications, Int. J. Biol. Macromol. 150 (2020) 1072–1083.
[148] Y. Liu, et al., An injectable, self-healing phenol-functionalized chitosan hydrogel with fast gelling property and visible light-crosslinking capability for 3D printing, Acta Biomater. 122 (2021) 211–219.
[149] S. Ahmed, S. Ikram, Chitosan based scaffolds and their applications in wound healing, Achievements in the Life Sciences 10 (2016) 27–37.
[150] P. Zucca, R. Fernandez-Lafuente, E. Sanjust, Agarose and its derivatives as supports for enzyme immobilization, Molecules 21 (11) (2016) 1577.
[151] A. Awadhiya, D. Kumar, V. Verma, Crosslinking of agarose bioplastic using citric acid, Carbohydrate Polym. 151 (2016) 60–67.
[152] G.R. López-Marcial, et al., Agarose-based hydrogels as suitable bioprinting materials for tissue engineering, ACS Biomater. Sci. Eng. 4 (10) (2018) 3610–3616.
[153] M. Tako, S. Nakamura, Gelation mechanism of agarose, Carbohydr. Res. 180 (2) (1988) 277–284.
[154] K.Y. Lee, D.J. Mooney, Hydrogels for tissue engineering, Chem. Rev. 101 (7) (2001) 1869–1880.
[155] A. Forget, et al., Mechanically tunable bioink for 3D bioprinting of human cells, Advanced Healthcare Materials 6 (20) (2017), 1700255.
[156] A. Nadernezhad, et al., Nanocomposite bioinks based on agarose and 2D nanosilicates with tunable flow properties and bioactivity for 3D bioprinting, ACS Appl. Bio Mater. 2 (2) (2019) 796–806.
[157] C. Gong, Z. Kong, X. Wang, The effect of agarose on 3D bioprinting, Polymers 13 (22) (2021) 4028.
[158] Z. Fu, et al., Responsive biomaterials for 3D bioprinting: a review, Mater. Today 52 (2022) 112–132.
[159] P. Zarrintaj, et al., Agarose-based biomaterials for tissue engineering, Carbohydrate Polym. 187 (2018) 66–84.
[160] A. Fakhari, C. Berkland, Applications and emerging trends of hyaluronic acid in tissue engineering, as a dermal filler and in osteoarthritis treatment, Acta Biomater. 9 (7) (2013) 7081–7092.
[161] M.K. Paap, R.Z. Silkiss, The interaction between hyaluronidase and hyaluronic acid gel fillers-a review of the literature and comparative analysis, Plastic and Aesthetic Research 7 (2020) 36.
[162] S. Khunmanee, Y. Jeong, H. Park, Crosslinking method of hyaluronic-based hydrogel for biomedical applications, J. Tissue Eng. 8 (2017), 2041731417726464.
[163] J. Kim, et al., Bone regeneration using hyaluronic acid-based hydrogel with bone morphogenic protein-2 and human mesenchymal stem cells, Biomaterials 28 (10) (2007) 1830–1837.
[164] Z. Zhu, et al., Hyaluronic acid: a versatile biomaterial in tissue engineering, Plastic and Aesthetic Research 4 (2017) 219–227.
[165] N. Ashammakhi, et al., Advancing frontiers in bone bioprinting, Advanced Healthcare Materials 8 (7) (2019), 1801048.
[166] P. Zhai, et al., The application of hyaluronic acid in bone regeneration, Int. J. Biol. Macromol. 151 (2020) 1224–1239.
[167] N. Law, et al., Characterisation of hyaluronic acid methylcellulose hydrogels for 3D bioprinting, J. Mech. Behav. Biomed. Mater. 77 (2018) 389–399.
[168] L. Ouyang, et al., 3D printing of shear-thinning hyaluronic acid hydrogels with secondary cross-linking, ACS Biomater. Sci. Eng. 2 (10) (2016) 1743–1751.
[169] A. Fallacara, et al., Hyaluronic acid in the third millennium, Polymers 10 (7) (2018) 701.
[170] A.D. Doyle, Generation of 3D collagen gels with controlled diverse architectures, Current protocols in cell biology 72 (1) (2016), 10.20. 1-10.20. 16.
[171] W.T. Brinkman, et al., Photo-cross-linking of type I collagen gels in the presence of smooth muscle cells: mechanical properties, cell viability, and function, Biomacromolecules 4 (4) (2003) 890–895.
[172] S. Rhee, et al., 3D bioprinting of spatially heterogeneous collagen constructs for cartilage tissue engineering, ACS Biomater. Sci. Eng. 2 (10) (2016) 1800–1805.
[173] M. Mohseni, et al., Assessment of tricalcium phosphate/collagen (TCP/collagene) nanocomposite scaffold compared with hydroxyapatite (HA) on healing of segmental femur bone defect in rabbits, Artif. Cell Nanomed. Biotechnol. 46 (2) (2018) 242–249.
[174] G. Turnbull, et al., 3D bioactive composite scaffolds for bone tissue engineering, Bioact. Mater. 3 (3) (2018) 278–314.
[175] N. Xu, et al., Marine-derived collagen as biomaterials for human Health, Front. Nutr. 8 (2021).
[176] Y. Wang, Z. Wang, Y. Dong, Collagen-based biomaterials for tissue engineering, ACS Biomater. Sci. Eng. 9 (3) (2023) 1132–1150.
[177] Y.B. Pottathara, et al., Solidification of gelatine hydrogels by using a cryoplatform and its validation through CFD approaches, Gels 8 (6) (2022) 368.
[178] C.E. Campiglio, et al., Cross-linking strategies for electrospun gelatin scaffolds, Materials 12 (15) (2019) 2476.
[179] S. Farzamfar, et al., Polycaprolactone/gelatin nanofibrous scaffolds for tissue engineering, Biointerface Res. Appl. Chem 11 (2020) 11104–11115.
[180] Y. Luo, et al., 3D printing of concentrated alginate/gelatin scaffolds with homogeneous nano apatite coating for bone tissue engineering, Mater. Des. 146 (2018) 12–19.
[181] Y. Luo, et al., Concentrated gelatin/alginate composites for fabrication of predesigned scaffolds with a favorable cell response by 3D plotting, RSC Adv. 5 (54) (2015) 43480–43488.
[182] L. Ouyang, et al., Void-free 3D bioprinting for in situ endothelialization and microfluidic perfusion, Adv. Funct. Mater. 30 (1) (2020), 1908349.
[183] L. Ouyang, et al., Expanding and optimizing 3D bioprinting capabilities using complementary network bioinks, Sci. Adv. 6 (38) (2020) eabc5529.
[184] L. Xiang, W. Cui, Biomedical application of photo-crosslinked gelatin hydrogels, Journal of Leather Science and Engineering 3 (1) (2021) 3.
[185] T.-C. Hua, B.-L. Liu, H. Zhang, Freeze-drying of Pharmaceutical and Food Products, Elsevier, 2010.
[186] J.W. Weisel, R.I. Litvinov, Mechanisms of fibrin polymerization and clinical implications, Blood, The Journal of the American Society of Hematology 121 (10) (2013) 1712–1719.
[187] E. Abelseth, et al., 3D printing of neural tissues derived from human induced pluripotent stem cells using a fibrin-based bioink, ACS Biomater. Sci. Eng. 5 (1) (2019) 234–243.
[188] B.A.G. de Melo, et al., Strategies to use fibrinogen as bioink for 3D bioprinting fibrin-based soft and hard tissues, Acta Biomater. 117 (2020) 60–76.
[189] J. Arulmoli, et al., Combination scaffolds of salmon fibrin, hyaluronic acid, and laminin for human neural stem cell and vascular tissue engineering, Acta Biomater. 43 (2016) 122–138.
[190] C.H.B. Reis, et al., Application of fibrin associated with photobiomodulation as a promising strategy to improve regeneration in tissue engineering: a systematic review, Polymers 14 (15) (2022) 3150.
[191] E. Sproul, S. Nandi, A. Brown, 6 - fibrin biomaterials for tissue regeneration and repair, in: M.A. Barbosa, M.C.L. Martins (Eds.), Peptides and Proteins as Biomaterials for Tissue Regeneration and Repair, Woodhead Publishing, 2018, pp. 151–173.
[192] S. Lee, X. Tong, F. Yang, Effects of the poly (ethylene glycol) hydrogel crosslinking mechanism on protein release, Biomater. Sci. 4 (3) (2016) 405–411.
[193] Z.A. Hamid, K. Lim, Evaluation of UV-crosslinked poly (ethylene glycol) diacrylate/poly (dimethylsiloxane) dimethacrylate hydrogel: properties for tissue engineering application, Procedia Chem. 19 (2016) 410–418.
[194] J. Bai, et al., Melt electrohydrodynamic 3D printed poly (ε-caprolactone)/polyethylene glycol/roxithromycin scaffold as a potential anti-infective implant in bone repair, Int. J. Pharm. 576 (2020), 118941.
[195] G. Burke, et al., Evaluation of the materials properties, stability and cell response of a range of PEGDMA hydrogels for tissue engineering applications, J. Mech. Behav. Biomed. Mater. 99 (2019) 1–10.
[196] Z. Chen, et al., 3D printing of multifunctional hydrogels, Adv. Funct. Mater. 29 (20) (2019), 1900971.
[197] M.-Y. Shie, et al., 3D printing of cytocompatible water-based light-cured polyurethane with hyaluronic acid for cartilage tissue engineering applications, Materials 10 (2) (2017) 136.
[198] X. Yao, et al., Poly(ethylene glycol) alternatives in biomedical applications, Nano Today 48 (2023), 101738.
[199] Y. Yang, et al., Synthesis of aligned porous polyethylene glycol/silk fibroin/hydroxyapatite scaffolds for osteoinduction in bone tissue engineering, Stem Cell Res. Ther. 11 (1) (2020) 522.
[200] J. Fan, et al., High protein content keratin/poly (ethylene oxide) nanofibers crosslinked in oxygen atmosphere and its cell culture, Mater. Des. 104 (2016) 60–67.
[201] D. Singh, P.H. Huh, S.C. Kim, Hyperbranched poly (glycidol)/poly (ethylene oxide) crosslinked hydrogel for tissue engineering scaffold using e-beams, J. Biomed. Mater. Res. 104 (1) (2016) 48–56.
[202] L. Viidik, et al., 3D-printability of aqueous poly(ethylene oxide) gels, Eur. Polym. J. 120 (2019), 109206.
[203] F. Liu, X. Wang, Synthetic polymers for organ 3D printing, Polymers 12 (8) (2020) 1765.
[204] H. Nosrati, et al., Preparation and characterization of poly(ethylene oxide)/zinc oxide nanofibrous scaffold for chronic wound healing applications, Polim. Med. 50 (1) (2020) 41–51.
[205] F. Habibzadeh, et al., Nanomaterials supported by polymers for tissue engineering applications: a review, Heliyon 8 (12) (2022), e12193.
[206] F. Boschetto, et al., Antibacterial and osteoconductive effects of chitosan/polyethylene oxide (PEO)/Bioactive glass nanofibers for orthopedic applications, Appl. Sci. 10 (7) (2020) 2360.
[207] M.U. Minhas, et al., Synthesis of chemically cross-linked polyvinyl alcohol-co-poly (methacrylic acid) hydrogels by copolymerization; a potential graft-polymeric carrier for oral delivery of 5-fluorouracil, Daru 21 (1) (2013) 1–9.

[208] F. Yokoyama, et al., Morphology and structure of highly elastic poly (vinyl alcohol) hydrogel prepared by repeated freezing-and-melting, Colloid Polym. Sci. 264 (7) (1986) 595–601.
[209] J. Maitra, V.K. Shukla, Cross-linking in hydrogels-a review, Am. J. Polym. Sci. 4 (2) (2014) 25–31.
[210] M. Goldvaser, et al., Poly(vinyl alcohol)-methacrylate with CRGD peptide: a photocurable biocompatible hydrogel, J Tissue Eng Regen Med 16 (2) (2022) 140–150.
[211] L. Gautam, et al., A review on carboxylic acid cross-linked polyvinyl alcohol: properties and applications, Polym. Eng. Sci. 62 (2) (2022) 225–246.
[212] P.J. Martens, S.J. Bryant, K.S. Anseth, Tailoring the degradation of hydrogels formed from multivinyl poly(ethylene glycol) and poly(vinyl alcohol) macromers for cartilage tissue engineering, Biomacromolecules 4 (2) (2003) 283–292.
[213] C.-T. Lee, P.-H. Kung, Y.-D. Lee, Preparation of poly(vinyl alcohol)-chondroitin sulfate hydrogel as matrices in tissue engineering, Carbohydrate Polym. 61 (3) (2005) 348–354.
[214] M.A. Teixeira, M.T.P. Amorim, H.P. Felgueiras, Poly(Vinyl alcohol)-based nanofibrous electrospun scaffolds for tissue engineering applications, Polymers 12 (1) (2020) 7.
[215] I. Zulkiflee, M.B. Fauzi, Gelatin-polyvinyl alcohol film for tissue engineering: a concise review, Biomedicines 9 (8) (2021).
[216] Y. He, et al., An investigation of the behavior of solvent based polycaprolactone ink for material jetting, Sci. Rep. 6 (1) (2016) 1–10.
[217] J. Pal, et al., Control on molecular weight reduction of poly (ε-caprolactone) during melt spinning—a way to produce high strength biodegradable fibers, Mater. Sci. Eng. C 33 (7) (2013) 4213–4220.
[218] D. Zhao, et al., Effect of pore geometry on the fatigue properties and cell affinity of porous titanium scaffolds fabricated by selective laser melting, J. Mech. Behav. Biomed. Mater. 88 (2018) 478–487.
[219] H. Li, et al., A novel 3D printing PCL/GelMA scaffold containing USPIO for MRI-guided bile duct repair, Biomed. Mater. 15 (4) (2020), 045004.
[220] A. Kumar, et al., Load-bearing biodegradable PCL-PGA-beta TCP scaffolds for bone tissue regeneration, J. Biomed. Mater. Res. B Appl. Biomater. 109 (2) (2021) 193–200.
[221] N. Siddiqui, et al., Electropsun polycaprolactone fibres in bone tissue engineering: a review, Mol. Biotechnol. 63 (5) (2021) 363–388.
[222] R.A. Ilyas, et al., Natural fiber-reinforced polycaprolactone green and hybrid biocomposites for various advanced applications, Polymers 14 (1) (2022) 182.
[223] X. Yang, et al., The application of polycaprolactone in three-dimensional printing scaffolds for bone tissue engineering, Polymers 13 (16) (2021) 2754.
[224] P.R. Schmitt, K.D. Dwyer, K.L.K. Coulombe, Current applications of polycaprolactone as a scaffold material for heart regeneration, ACS Appl. Bio Mater. 5 (6) (2022) 2461–2480.
[225] S.-X. Yu, et al., Morphology control of PLA microfibers and spheres via melt electrospinning, Mater. Res. Express 5 (4) (2018), 045019.
[226] U. Sonchaeng, et al., In-situ changes of thermo-mechanical properties of poly (lactic acid) film immersed in alcohol solutions, Polym. Test. 82 (2020), 106320.
[227] M. Bednarek, K. Borska, P. Kubisa, Crosslinking of polylactide by high energy irradiation and photo-curing, Molecules 25 (21) (2020) 4919.
[228] S. Liu, et al., Current applications of poly(lactic acid) composites in tissue engineering and drug delivery, Compos. B Eng. 199 (2020), 108238.
[229] M.V. Granados-Hernández, et al., In vitro and in vivo biological characterization of poly(lactic acid) fiber scaffolds synthesized by air jet spinning, J. Biomed. Mater. Res. B Appl. Biomater. 106 (6) (2018) 2435–2446.
[230] K.M. Nampoothiri, N.R. Nair, R.P. John, An overview of the recent developments in polylactide (PLA) research, Bioresour. Technol. 101 (22) (2010) 8493–8501.
[231] N. Iqbal, et al., Recent concepts in biodegradable polymers for tissue engineering paradigms: a critical review, Int. Mater. Rev. 64 (2) (2019) 91–126.
[232] X. Lin, et al., Poly(Lactic acid)-based biomaterials: synthesis, modification and applications, in: N.G. Dhanjoo (Ed.), Biomedical Science, Engineering and Technology, IntechOpen: Rijeka, 2012. Ch. 11.
[233] F. Alam, et al., Microarchitected 3D printed polylactic acid (PLA) nanocomposite scaffolds for biomedical applications, J. Mech. Behav. Biomed. Mater. 103 (2020), 103576.
[234] J. Zhang, et al., Novel fabricating process for porous polyglycolic acid scaffolds by melt-foaming using supercritical carbon dioxide, ACS Biomater. Sci. Eng. 4 (2) (2018) 694–706.
[235] Y. Chen, et al., Fast-scanning chip-calorimetry measurement of crystallization kinetics of poly (glycolic acid), Polymers 13 (6) (2021) 891.
[236] S. Toosi, et al., PGA-incorporated collagen: toward a biodegradable composite scaffold for bone-tissue engineering, J. Biomed. Mater. Res. 104 (8) (2016) 2020–2028.
[237] S. Mhiri, et al., Thermally reversible and biodegradable polyglycolic-acid-based networks, Eur. Polym. J. 88 (2017) 292–310.
[238] E.D. Boland, et al., Tailoring tissue engineering scaffolds using electrostatic processing techniques: a study of poly(glycolic acid) electrospinning, J. Macromol. Sci., Part A 38 (12) (2001) 1231–1243.
[239] R. Liang, Y. Sun, J. Zhu, Applications of polymer materials in power industry, tissue engineering and fuel cells, Highlights in Science, Engineering and Technology 13 (2022) 190–197.
[240] S. Amiri, et al., Evaluation of polyglycolic acid as an animal-free biomaterial for three-dimensional culture of human endometrial cells, Clinical and Experimental Reproductive Medicine 49 (4) (2022) 259–269.
[241] Q. Zhang, et al., 3D printing method for bone tissue engineering scaffold, Medicine in Novel Technology and Devices 17 (2023), 100205.
[242] K. Budak, O. Sogut, U. Aydemir Sezer, A review on synthesis and biomedical applications of polyglycolic acid, J. Polym. Res. 27 (8) (2020) 208.
[243] X. Tian, et al., Characterization of the flow behavior of alginate/hydroxyapatite mixtures for tissue scaffold fabrication, Biofabrication 1 (4) (2009), 045005.
[244] X.Y. Tian, X.B. Chen, Effects of cell density on mechanical properties of alginate hydrogel tissue scaffolds, in: Journal of Biomimetics, Biomaterials and Tissue Engineering, Trans Tech Publ, 2014.
[245] Y. Yang, et al., Minimally invasive bioprinting for in situ liver regeneration, Bioact. Mater. 26 (2023) 465–477.
[246] X. Chen, M. Li, H. Ke, Modeling of the flow rate in the dispensing-based process for fabricating tissue scaffolds, J. Manuf. Sci. Eng. 130 (2) (2008).
[247] X. Chen, H. Ke, Effects of fluid properties on dispensing processes for electronics packaging, IEEE Trans. Electron. Packag. Manuf. 29 (2) (2006) 75–82.
[248] W. Hu, et al., Advances in crosslinking strategies of biomedical hydrogels, Biomater. Sci. 7 (3) (2019) 843–855.
[249] L. Sando, et al., Photochemically crosslinked matrices of gelatin and fibrinogen promote rapid cell proliferation, Journal of Tissue Engineering and Regenerative Medicine 5 (5) (2011) 337–346.
[250] Y. Zhou, et al., An injectable bioink with rapid prototyping in the air and in-situ mild polymerization for 3D bioprinting, Biofabrication 13 (4) (2021), 045026.
[251] S. Choi, H. Ahn, S.H. Kim, Tyrosinase-mediated hydrogel crosslinking for tissue engineering, J. Appl. Polym. Sci. 139 (14) (2022), 51887.
[252] J.B. Costa, et al., Fast setting silk fibroin bioink for bioprinting of patient-specific memory-shape implants, Advanced healthcare materials 6 (22) (2017), 1701021.
[253] E. Gantumur, et al., Extrusion-based bioprinting through glucose-mediated enzymatic hydrogelation, Int J Bioprint 6 (1) (2020) 250.
[254] H.M. El-Husseiny, et al., Smart/stimuli-responsive hydrogels: cutting-edge platforms for tissue engineering and other biomedical applications, Materials Today Bio 13 (2022), 100186.
[255] R. Naranjo-Alcazar, et al., Research progress in enzymatically cross-linked hydrogels as injectable systems for bioprinting and tissue engineering, Gels 9 (3) (2023) 230.
[256] F. Züger, N. Berner, M.R. Gullo, Towards a novel cost-effective and versatile bioink for 3D-bioprinting in tissue engineering, Biomimetics 8 (1) (2023) 27.
[257] R. Chaudhuri, et al., Biomaterials and cells for cardiac tissue engineering: current choices, Mater. Sci. Eng. C 79 (2017) 950–957.
[258] A.A. Shokeir, A.M. Harraz, A.B.S. El-Din, Tissue engineering and stem cells: basic principles and applications in urology, Int. J. Urol. 17 (12) (2010) 964–973.
[259] N. Bawolin, X. Chen, Remote determination of time-dependent stiffness of surface-degrading-polymer scaffolds via synchrotron-based imaging, J. Biomech. Eng. 139 (4) (2017).
[260] A.J. Engler, S. Sen, hl Sweeney, D.E. Discher, Matrix elasticity directs stem cell lineage specification, Cell 126 (2006) 677–689.
[261] A. Hayn, T. Fischer, C.T. Mierke, Inhomogeneities in 3D collagen matrices impact matrix mechanics and cancer cell migration, Front. Cell Dev. Biol. 8 (2020), 593879.
[262] M. Abdallah, et al., Influence of hydrolyzed polyacrylamide hydrogel stiffness on podocyte morphology, phenotype, and mechanical properties, ACS Appl. Mater. Interfaces 11 (36) (2019) 32623–32632.
[263] C.J. Little, N.K. Bawolin, X. Chen, Mechanical properties of natural cartilage and tissue-engineered constructs, Tissue Eng. B Rev. 17 (4) (2011) 213–227.
[264] B. Lee, et al., 3D micromesh-based hybrid bioprinting: multidimensional liquid patterning for 3D microtissue engineering, NPG Asia Mater. 14 (1) (2022) 6.
[265] J. Jang, et al., Effects of alginate hydrogel cross-linking density on mechanical and biological behaviors for tissue engineering, in: Journal of the Mechanical Behavior of Biomedical Materials, vol. 37, 2014, pp. 69–77.
[266] C.K. Kuo, P.X. Ma, Maintaining dimensions and mechanical properties of ionically crosslinked alginate hydrogel scaffolds in vitro, 4, in: Journal of Biomedical Materials Research Part A: an Official Journal of the Society for Biomaterials, the Japanese Society for Biomaterials, and the Australian Society for Biomaterials and the Korean Society for Biomaterials, vol. 84, 2008, pp. 899–907.
[267] S. Jana, et al., High-strength pristine porous chitosan scaffolds for tissue engineering, J. Mater. Chem. 22 (13) (2012) 6291–6299.
[268] Q. Xing, et al., Increasing mechanical strength of gelatin hydrogels by divalent metal ion removal, Sci. Rep. 4 (1) (2014) 1–10.
[269] M. Bertasa, et al., Agar gel strength: a correlation study between chemical composition and rheological properties, Eur. Polym. J. 123 (2020), 109442.
[270] V. Normand, et al., New insight into agarose gel mechanical properties, Biomacromolecules 1 (4) (2000) 730–738.
[271] S. Bose, et al., Dry vs. wet: properties and performance of collagen films. Part I. Mechanical behaviour and strain-rate effect, J. Mech. Behav. Biomed. Mater. 111 (2020), 103983.
[272] J. Lee, et al., Effect of chain flexibility on cell adhesion: semi-flexible model-based analysis of cell adhesion to hydrogels, Sci. Rep. 9 (1) (2019) 2463.
[273] F. Della Sala, et al., Mechanical behavior of bioactive poly (ethylene glycol) diacrylate matrices for biomedical application, J. Mech. Behav. Biomed. Mater. 110 (2020), 103885.
[274] D. Husken, R. Gaymans, The tensile properties of poly (ethylene oxide)-based segmented block copolymers in the dry and wet state, J. Mater. Sci. 44 (2009) 2656–2664.
[275] B.H. Musa, N.J. Hameed, Study of the mechanical properties of polyvinyl alcohol/starch blends, Mater. Today Proc. 20 (2020) 439–442.
[276] J. Zhang, et al., Enhancing the thermal and mechanical properties of polyvinyl alcohol (PVA) with boron nitride nanosheets and cellulose nanocrystals, Polymer 148 (2018) 101–108.

[277] M. Wang, et al., Poly (sodium 4-styrenesulfonate) modified graphene for reinforced biodegradable poly (ε-caprolactone) nanocomposites, RSC Adv. 5 (89) (2015) 73146–73154.
[278] S. Kumar, S. Bose, K. Chatterjee, Amine-functionalized multiwall carbon nanotubes impart osteoinductive and bactericidal properties in poly (ε-caprolactone) composites, RSC Adv. 4 (37) (2014) 19086–19098.
[279] J.M. Reverte, et al., Mechanical and geometric performance of PLA-based polymer composites processed by the fused filament fabrication additive manufacturing technique, Materials 13 (8) (2020) 1924.
[280] B.A. Aloyaydi, S. Sivasankaran, Low-velocity impact characteristics of 3D-printed poly-lactic acid thermoplastic processed by fused deposition modeling, Trans. Indian Inst. Met. 73 (2020) 1669–1677.
[281] D. Oravec, et al., The relationship of whole human vertebral body creep to bone density and texture via clinically available imaging modalities, J. Biomech. 135 (2022), 111021.
[282] A.K. Miri, et al., Nanoscale viscoelasticity of extracellular matrix proteins in soft tissues: a multiscale approach, J. Mech. Behav. Biomed. Mater. 30 (2014) 196–204.
[283] S. Javid, A. Rezaei, G. Karami, A micromechanical procedure for viscoelastic characterization of the axons and ECM of the brainstem, J. Mech. Behav. Biomed. Mater. 30 (2014) 290–299.
[284] S. Nam, et al., Varying PEG Density to Control Stress Relaxation in Alginate-PEG Hydrogels for 3D Cell Culture Studies, vol. 200, Biomaterials, 2019, pp. 15–24.
[285] Z. Fu, et al., Printability in extrusion bioprinting, Biofabrication 13 (3) (2021), 033001.
[286] A. Malekpour, X. Chen, Printability and cell viability in extrusion-based bioprinting from experimental, computational, and machine learning views, J. Funct. Biomater. 13 (2) (2022) 40.
[287] M. Li, et al., Modeling process-induced cell damage in the biodispensing process, Tissue Eng. C Methods 16 (3) (2010) 533–542.
[288] L. Ning, et al., Characterization of cell damage and proliferative ability during and after bioprinting, ACS Biomater. Sci. Eng. 4 (11) (2018) 3906–3918.
[289] M. Li, et al., Modeling mechanical cell damage in the bioprinting process employing a conical needle, J. Mech. Med. Biol. 15 (5) (2015), 1550073.
[290] M.G. Li, X.Y. Tian, X. Chen, Temperature effect on the shear-induced cell damage in biofabrication, Artif. Organs 35 (7) (2011) 741–746.
[291] M. Li, et al., Effect of needle geometry on flow rate and cell damage in the dispensing-based biofabrication process, Biotechnol. Prog. 27 (6) (2011) 1777–1784.
[292] M. Li, X. Tian, X. Chen, Modeling of flow rate, pore size, and porosity for the dispensing-based tissue scaffolds fabrication, J. Manuf. Sci. Eng. 131 (3) (2009).
[293] X. Chen, Time-dependent Rheological Behavior of Fluids for Electronics Packaging, 2005.
[294] L.A. Down, D.V. Papavassiliou, E.A. O'Rear, Significance of extensional stresses to red blood cell lysis in a shearing flow, Ann. Biomed. Eng. 39 (6) (2011) 1632–1642.
[295] F. Cogswell, Measuring the extensional rheology of polymer melts, Trans. Soc. Rheol. 16 (3) (1972) 383–403.
[296] H. Xu, et al., Prediction of cell viability in dynamic optical projection stereolithography-based bioprinting using machine learning, J. Intell. Manuf. (2022) 1–11.
[297] C. Liu, et al., Computer vision-aided bioprinting for bone research, Bone Research 10 (1) (2022) 21.
[298] A.C. Daly, et al., A comparison of different bioinks for 3D bioprinting of fibrocartilage and hyaline cartilage, Biofabrication 8 (4) (2016), 045002.
[299] N.T. Raveendran, et al., Optimization of 3D bioprinting of periodontal ligament cells, Dent. Mater. 35 (12) (2019) 1683–1694.
[300] K.K. Moncal, et al., Thermally-controlled extrusion-based bioprinting of collagen, J. Mater. Sci. Mater. Med. 30 (2019) 1–14.
[301] B.-k. Wang, et al., Study on the 3D BioPrinting technology of hydrogel tissue engineering scaffolds, in: Journal of Physics: Conference Series, IOP Publishing, 2022.
[302] S. Ahn, G. Kim, Cell-encapsulating alginate microsized beads using an air-assisted atomization process to obtain a cell-laden hybrid scaffold, J. Mater. Chem. B 3 (47) (2015) 9132–9139.
[303] L. Ning, X. Chen, A brief review of extrusion-based tissue scaffold bio-printing, Biotechnol. J. 12 (8) (2017), 1600671.
[304] Z. Izadifar, et al., Analyzing Biological Performance of 3D-Printed, Cell-Impregnated Hybrid Constructs for Cartilage Tissue Engineering, Tissue Engineering, 2015 (ja).
[305] L. Ouyang, et al., Effect of bioink properties on printability and cell viability for 3D bioplotting of embryonic stem cells, Biofabrication 8 (3) (2016), 035020.
[306] G. Singh, et al., Advances in additive manufacturing techniques for bioprinting, ECS Trans. 107 (1) (2022) 6273.
[307] L. Ning, et al., 3D bioprinting of scaffolds with living Schwann cells for potential nerve tissue engineering applications, Biofabrication 10 (3) (2018), 035014.
[308] Z. Li, et al., Tuning alginate-gelatin bioink properties by varying solvent and their impact on stem cell behavior, Sci. Rep. 8 (1) (2018) 8020.
[309] N. Paxton, et al., Proposal to assess printability of bioinks for extrusion-based bioprinting and evaluation of rheological properties governing bioprintability, Biofabrication 9 (4) (2017), 044107.
[310] A. Kostenko, S. Swioklo, C.J. Connon, Effect of calcium sulphate pre-crosslinking on rheological parameters of alginate based bio-inks and on human corneal stromal fibroblast survival in 3D bio-printed constructs, Front. Mech. Eng. 8 (2022) 21.
[311] J. Hazur, et al., Improving alginate printability for biofabrication: establishment of a universal and homogeneous pre-crosslinking technique, Biofabrication 12 (4) (2020), 045004.
[312] L. Ouyang, et al., A generalizable strategy for the 3D bioprinting of hydrogels from nonviscous photo-crosslinkable inks, Adv. Mater. 29 (8) (2017), 1604983.
[313] L. Ning, et al., A 3D bioprinted in vitro model of neuroblastoma recapitulates dynamic tumor-endothelial cell interactions contributing to solid tumor aggressive behavior, Adv. Sci. (2022), 2200244.
[314] F. Meng, et al., 3D bioprinted in vitro metastatic models via reconstruction of tumor microenvironments, Adv. Mater. 31 (10) (2019), 1806899.
[315] S. Naghieh, X. Chen, Printability–A key issue in extrusion-based bioprinting, Journal of Pharmaceutical Analysis 11 (5) (2021) 564–579.
[316] C. O'Connell, et al., Characterizing bioinks for extrusion bioprinting: printability and rheology, 3D Bioprinting: Principles and Protocols (2020) 111–133.
[317] P. Xu, et al., Development of a quantitative method to evaluate the printability of filaments for fused deposition modeling 3D printing, Int. J. Pharm. 588 (2020), 119760.
[318] F. You, et al., Bioprinting and in vitro characterization of alginate dialdehyde–gelatin hydrogel bio-ink, Bio-Design and Manufacturing 3 (2020) 48–59.
[319] A. Schwab, et al., Printability and shape fidelity of bioinks in 3D bioprinting, Chem. Rev. 120 (19) (2020) 11028–11055.
[320] A. GhavamiNejad, et al., Crosslinking strategies for 3D bioprinting of polymeric hydrogels, Small 16 (35) (2020), 2002931.
[321] T. Gao, et al., Optimization of gelatin–alginate composite bioink printability using rheological parameters: a systematic approach, Biofabrication 10 (3) (2018), 034106.
[322] A. Fatimi, et al., Natural hydrogel-based bio-inks for 3D bioprinting in tissue engineering: a review, Gels 8 (3) (2022) 179.
[323] S. Raees, et al., Classification, processing, and applications of bioink and 3D bioprinting: a detailed review, Int. J. Biol. Macromol. (2023), 123476.
[324] Y. Gu, A. Forget, V.P. Shastri, Biobridge: an outlook on translational bioinks for 3D bioprinting, Adv. Sci. 9 (3) (2022), 2103469.
[325] Z. Heydari, et al., Mimicking the Liver Function in Micro-patterned Units: Challenges and Perspectives in 3D-Bioprinting, Bioprinting, 2022, e00208.
[326] M. Klak, et al., Bioink based on the dECM for 3D bioprinting of bionic tissue, the first results obtained on murine model, Bioprinting 28 (2022), e00233.
[327] A. Passaniti, H.K. Kleinman, G.R. Martin, Matrigel: history/background, uses, and future applications, Journal of Cell Communication and Signaling 16 (4) (2022) 621–626.
[328] S. Kim, et al., Tissue extracellular matrix hydrogels as alternatives to Matrigel for culturing gastrointestinal organoids, Nat. Commun. 13 (1) (2022) 1692.
[329] J. van der Valk, Fetal bovine serum—a cell culture dilemma, Science 375 (6577) (2022) 143–144.
[330] Z. Onódi, et al., Systematic transcriptomic and phenotypic characterization of human and murine cardiac myocyte cell lines and primary cardiomyocytes reveals serious limitations and low resemblances to adult cardiac phenotype, J. Mol. Cell. Cardiol. 165 (2022) 19–30.
[331] A. Persaud, et al., 3D Bioprinting with Live Cells, Engineered Regeneration, 2022.
[332] A. Joshi, T. Kaur, N. Singh, 3D bioprinted alginate-silk-based smart cell-instructive scaffolds for dual differentiation of human mesenchymal stem cells, ACS Appl. Bio Mater. 5 (6) (2022) 2870–2879.
[333] I. Roato, et al., Challenges of periodontal tissue engineering: increasing biomimicry through 3D printing and controlled dynamic environment, Nanomaterials 12 (21) (2022) 3878.
[334] G. Liu, et al., A 3D-printed biphasic calcium phosphate scaffold loaded with platelet lysate/gelatin methacrylate to promote vascularization, J. Mater. Chem. B 10 (16) (2022) 3138–3151.
[335] S.G. Anthon, K.P. Valente, Vascularization strategies in 3D cell culture models: from scaffold-free models to 3D bioprinting, Int. J. Mol. Sci. 23 (23) (2022), 14582.
[336] G.G. Chan, C.M. Koch, L.H. Connors, Blood proteomic profiling in inherited (ATTRm) and acquired (ATTRwt) forms of transthyretin-associated cardiac amyloidosis, J. Proteome Res. 16 (4) (2017) 1659–1668.
[337] M. Shen, et al., 3D bioprinting of in situ vascularized tissue engineered bone for repairing large segmental bone defects, Materials Today Bio 16 (2022), 100382.
[338] T. Zandrini, et al., Breaking the resolution limits of 3D bioprinting: future opportunities and present challenges, Trend Biotechnol. 41 (5) (2022) 604–614.
[339] E.H.Y. Lam, et al., 3D bioprinting for next-generation personalized medicine, Int. J. Mol. Sci. 24 (7) (2023) 6357.
[340] K. Nair, et al., Characterization of cell viability during bioprinting processes, Biotechnol. J.: Healthcare Nutrition Technology 4 (8) (2009) 1168–1177.
[341] Y. Fang, et al., Advances in 3D bioprinting, in: Chinese Journal of Mechanical Engineering: Additive Manufacturing Frontiers, 2022, 100011.
[342] Z. Li, et al., Modular-based gradient scaffold design and experimental studies for tissue engineering: enabling customized structures and mechanical properties, J. Mater. Sci. 57 (36) (2022) 17398–17415.
[343] Z. Izadifar, X. Chen, W. Kulyk, Strategic design and fabrication of engineered scaffolds for articular cartilage repair, J. Funct. Biomater. 3 (4) (2012) 799–838.
[344] M. Sarker, et al., Regeneration of peripheral nerves by nerve guidance conduits: influence of design, biopolymers, cells, growth factors, and physical stimuli, Prog. Neurobiol. 171 (2018) 125–150.
[345] F. Mohabatpour, et al., Novel Trends, Challenges and New Perspectives for Enamel Repair and Regeneration to Treat Dental Defects, Biomaterials Science, 2022.

[346] T.-C. Cham, X. Chen, A. Honaramooz, Current progress, challenges, and future prospects of testis organoids, Biol. Reprod. 104 (5) (2021) 942–961.
[347] S. Naghieh, et al., Dispensing-based bioprinting of mechanically-functional hybrid scaffolds with vessel-like channels for tissue engineering applications–a brief review, J. Mech. Behav. Biomed. Mater. 78 (2018) 298–314.
[348] A. Rajaram, X.-B. Chen, D.J. Schreyer, Strategic design and recent fabrication techniques for bioengineered tissue scaffolds to improve peripheral nerve regeneration, Tissue Eng. B Rev. 18 (6) (2012) 454–467.
[349] S. Liu, et al., Synergistic angiogenesis promoting effects of extracellular matrix scaffolds and adipose-derived stem cells during wound repair, Tissue Eng. 17 (5–6) (2011) 725–739.
[350] M.H. Sehhat, et al., Plasma spheroidization of gas-atomized 304L stainless steel powder for laser powder bed fusion process, Materials Science in Additive Manufacturing 1 (1) (2022) 1.
[351] O.A. Hamid, et al., 3D bioprinting of a stem cell-laden, multi-material tubular composite: an approach for spinal cord repair, Mater. Sci. Eng. C 120 (2021), 111707.
[352] Z. Izadifar, et al., Analyzing biological performance of 3D-printed, cell-impregnated hybrid constructs for cartilage tissue engineering, Tissue Eng. C Methods 22 (3) (2016) 173–188.
[353] C. Nelson, S. Tuladhar, M.A. Habib, Designing an interchangeable multi-material nozzle system for 3D bioprinting process, in: International Manufacturing Science and Engineering Conference, American Society of Mechanical Engineers, 2021.
[354] F. Shahabipour, et al., Coaxial 3D bioprinting of tri-polymer scaffolds to improve the osteogenic and vasculogenic potential of cells in co-culture models, J. Biomed. Mater. Res. 110 (5) (2022) 1077–1089.
[355] S. Hong, et al., Coaxial bioprinting of cell-laden vascular constructs using a gelatin–tyramine bioink, Biomater. Sci. 7 (11) (2019) 4578–4587.
[356] L. Lian, et al., Uniaxial and coaxial vertical embedded extrusion bioprinting, Advanced healthcare materials 11 (9) (2022), 2102411.
[357] Y. Yu, et al., Dual-core coaxial bioprinting of double-channel constructs with a potential for perfusion and interaction of cells, Biofabrication 14 (3) (2022), 035012.
[358] E.J. Bolívar-Monsalve, et al., Continuous chaotic bioprinting of skeletal muscle-like constructs, Bioprinting 21 (2021), e00125.
[359] E.J. Bolívar-Monsalve, et al., One-step bioprinting of multi-channel hydrogel filaments using chaotic advection: fabrication of pre-vascularized muscle-like tissues, Advanced Healthcare Materials (2022), 2200448.
[360] M. Rocca, et al., Embedded multimaterial extrusion bioprinting, SLAS TECHNOLOGY: Translating Life Sciences Innovation 23 (2) (2018) 154–163.
[361] N. Betancourt, X. Chen, Review of extrusion-based multi-material bioprinting processes, Bioprinting 25 (2022), e00189.
[362] D. Kang, et al., Pre-set extrusion bioprinting for multiscale heterogeneous tissue structure fabrication, Biofabrication 10 (3) (2018), 035008.
[363] A. Colly, et al., Classification of the emerging freeform three-dimensional printing techniques, MRS Bull. (2022) 1–24.
[364] Y. Fang, et al., Expanding embedded 3D bioprinting capability for engineering complex organs with freeform vascular networks, Adv. Mater. (2023), 2205082.
[365] L. Ning, et al., Embedded 3D bioprinting of gelatin methacryloyl-based constructs with highly tunable structural fidelity, ACS Appl. Mater. Interfaces 12 (40) (2020) 44563–44577.
[366] A. Lee, et al., 3D bioprinting of collagen to rebuild components of the human heart, Science 365 (6452) (2019) 482–487.
[367] Y.-S. Chen, et al., Additive manufacturing of Schwann cell-laden collagen/alginate nerve guidance conduits by freeform reversible embedding regulate neurogenesis via exosomes secretion towards peripheral nerve regeneration, Biomaterials Advances (2023), 213276.
[368] Y. Zhu, et al., Three-dimensional bioprinting with alginate by freeform reversible embedding of suspended hydrogels with tunable physical properties and cell proliferation, Bioengineering 9 (12) (2022) 807.
[369] C.A. Wu, et al., Optimization of freeform reversible embedding of suspended hydrogel microspheres for substantially improved three-dimensional bioprinting capabilities, Tissue Eng. C Methods 29 (3) (2023) 85–94.
[370] L. Ning, et al., Biomechanical factors in three-dimensional tissue bioprinting, Appl. Phys. Rev. 7 (4) (2020), 041319.
[371] X. Zeng, et al., Embedded bioprinting for designer 3D tissue constructs with complex structural organization, Acta Biomater. 140 (2022) 1–22.
[372] F. Liu, et al., Hybrid biomanufacturing systems applied in tissue regeneration, International Journal of Bioprinting 9 (1) (2022).
[373] D.L. Yang, et al., Combination of 3D printing and electrospinning techniques for biofabrication, Advanced Materials Technologies 7 (7) (2022), 2101309.
[374] A. Sadeghianmaryan, et al., Electrospinning of polyurethane/graphene oxide for skin wound dressing and its in vitro characterization, J. Biomater. Appl. 35 (1) (2020) 135–145.
[375] A. Sadeghianmaryan, et al., Electrospinning of scaffolds from the polycaprolactone/polyurethane composite with graphene oxide for skin tissue engineering, Appl. Biochem. Biotechnol. 191 (2) (2020) 567–578.
[376] A. Gonzalez-Pujana, et al., Hybrid 3D printed and electrospun multi-scale hierarchical polycaprolactone scaffolds to induce bone differentiation, Pharmaceutics 14 (12) (2022) 2843.
[377] M. Namhongsa, et al., Surface-modified polypyrrole-coated PLCL and PLGA nerve guide conduits fabricated by 3D printing and electrospinning, Biomacromolecules 23 (11) (2022) 4532–4546.
[378] I. Mayoral González, et al., Tissue engineered in-vitro vascular patch fabrication using hybrid 3D printing and electrospinning, Materials Today Bio 14 (2022), 100252.
[379] J. Chen, et al., Promotion of skin regeneration through co-axial electrospun fibers loaded with basic fibroblast growth factor, Adv. Compos. Hybrid Mater. 5 (2) (2022) 1111–1125.
[380] Q. Yao, et al., Long-term induction of endogenous BMPs growth factor from antibacterial dual network hydrogels for fast large bone defect repair, J. Colloid Interface Sci. 607 (2022) 1500–1515.
[381] Y. Hao, et al., Carboxymethyl chitosan-based hydrogels containing fibroblast growth factors for triggering diabetic wound healing, Carbohydrate Polym. 287 (2022), 119336.
[382] P. Zhai, X.B. Chen, D.J. Schreyer, Preparation and characterization of alginate microspheres for sustained protein delivery within tissue scaffolds, Biofabrication 5 (1) (2013), 015009.
[383] R. Fang, et al., Sustained co-delivery of BIO and IGF-1 by a novel hybrid hydrogel system to stimulate endogenous cardiac repair in myocardial infarcted rat hearts, Int. J. Nanomed. 10 (2015) 4691–4703.
[384] P. Zhai, X.B. Chen, D.J. Schreyer, PLGA/alginate composite microspheres for hydrophilic protein delivery, Mater. Sci. Eng. C 56 (2015) 251–259.
[385] P. Zhai, X.B. Chen, D.J. Schreyer, An in vitro study of peptide-loaded alginate nanospheres for antagonizing the inhibitory effect of Nogo-A protein on axonal growth, Biomed. Mater. 10 (4) (2015), 045016.
[386] M. Izadifar, et al., Rate-programming of nano-particulate delivery systems for smart bioactive scaffolds in tissue engineering, Nanotechnology 26 (1) (2015), 012001.
[387] M. Izadifar, et al., Optimization of nanoparticles for cardiovascular tissue engineering, Nanotechnology 26 (23) (2015), 235301.
[388] M. Izadifar, M.E. Kelly, X. Chen, Regulation of sequential release of growth factors using bilayer polymeric nanoparticles for cardiac tissue engineering, Nanomedicine 11 (24) (2016) 3237–3259.
[389] M. Izadifar, M.E. Kelly, X. Chen, Computational nanomedicine for mechanistic elucidation of bilayer nanoparticle-mediated release for tissue engineering, Nanomedicine 12 (5) (2017) 423–442.
[390] F. Mohabatpour, et al., Gemini surfactant-based nanoparticles T-box1 gene delivery as a novel approach to promote epithelial stem cells differentiation and dental enamel formation, Biomaterials Advances 137 (2022), 212844.
[391] M. Izadifar, M.E. Kelly, X. Chen, Engineering angiogenesis for myocardial infarction repair: recent developments, challenges, and future directions, Cardiovascular Engineering and Technology 5 (4) (2014) 281–307.
[392] M. Sarker, et al., Bioprinting of vascularized tissue scaffolds: influence of biopolymer, cells, growth factors, and gene delivery 2019, J. Healthcare Eng. 2019 (2019) 1–20.
[393] M. Sarker, X. Chen, D. Schreyer, Experimental approaches to vascularisation within tissue engineering constructs, J. Biomater. Sci. Polym. Ed. 26 (12) (2015) 683–734.
[394] M.D. Sarker, et al., 3D biofabrication of vascular networks for tissue regeneration: a report on recent advances, Journal of Pharmaceutical Analysis 8 (5) (2018) 277–296.
[395] R.I. Ibanez, et al., 3D printed scaffolds incorporated with platelet-rich plasma show enhanced angiogenic potential while not inducing fibrosis, Adv. Funct. Mater. 32 (10) (2022), 2109915.
[396] Y. Kang, et al., 3D bioprinting of dECM/Gel/QCS/nHAp hybrid scaffolds laden with mesenchymal stem cell-derived exosomes to improve angiogenesis and osteogenesis, Biofabrication 15 (2) (2023), 024103.
[397] A.A. Szklanny, et al., 3D bioprinting of engineered tissue flaps with hierarchical vessel networks (VesselNet) for direct host-to-implant perfusion, Adv. Mater. 33 (42) (2021), 2102661.
[398] H.M. Eltaher, et al., Human-scale tissues with patterned vascular networks by additive manufacturing of sacrificial sugar-protein composites, Acta Biomater. 113 (2020) 339–349.
[399] C. Yu, J. Jiang, A perspective on using machine learning in 3D bioprinting, International Journal of Bioprinting 6 (1) (2020).
[400] J. An, C.K. Chua, V. Mironov, Application of machine learning in 3D bioprinting: focus on development of big data and digital twin, International journal of bioprinting 7 (1) (2021).
[401] W.L. Ng, et al., Deep learning for fabrication and maturation of 3D bioprinted tissues and organs, Virtual Phys. Prototyp. 15 (3) (2020) 340–358.
[402] K. Ruberu, et al., Coupling machine learning with 3D bioprinting to fast track optimisation of extrusion printing, Appl. Mater. Today 22 (2021), 100914.